

DOE/NASA/3277-1
NASA CR-159856
WER-10

**DO NOT DESTROY
RETURN TO LIBRARY**

FEASIBILITY STUDY OF AILERON AND SPOILER CONTROL SYSTEMS FOR LARGE HORIZONTAL AXIS WIND TURBINES

W.H. Wentz, Jr., M.H. Snyder,
and J.T. Calhoun
Wichita State University

May 1980

Prepared for
NATIONAL AERONAUTICS AND SPACE ADMINISTRATION
Lewis Research Center
Under Grant 3277

AUG 1980
MCDONNELL DOUGLAS
RESEARCH & ENGINEERING LIBRARY
ST. LOUIS

Prepared for
U.S. DEPARTMENT OF ENERGY
Energy Technology
Distributed Solar Technology Division

MRD-14810

NASA-CR-159856

1

NOTICE

This report was prepared to document work sponsored by the United States Government. Neither the United States nor its agent, the United States Department of Energy, nor any Federal employees, nor any of their contractors, subcontractors or their employees, makes any warranty, express or implied, or assumes any legal liability or responsibility for the accuracy, completeness, or usefulness of any information, apparatus, product or process disclosed, or represents that its use would not infringe privately owned rights.

DOE/NASA/1044-6
NASA CR-159856
WER-10

FEASIBILITY STUDY OF AILERON AND SPOILER CONTROL SYSTEMS FOR LARGE HORIZONTAL AXIS WIND TURBINES

W.H. Wentz, Jr., M.H. Synder,
and J.T. Calhoun
Wichita State University
Wichita, Kansas 67208

May 1980

Prepared for
National Aeronautics and Space Administration
Lewis Research Center
Cleveland, Ohio 44135
Under Grant 3277

for
U.S. DEPARTMENT OF ENERGY
Energy Technology
Distributed Solar Technology Division
Washington, D.C. 20545
Under Interagency Agreement EX-76-I-01-1028

TABLE OF CONTENTS

	<u>page</u>
SUMMARY.....	1
INTRODUCTION.....	2
PRELIMINARY CONSIDERATIONS.....	2
Control System Options Studied.....	2
Ailerons.....	3
Spoiler Type.....	3
Spoiler Hingeline Location.....	3
PERFORMANCE ANALYSIS.....	4
Leading-Edge Suction Studies.....	4
Single Point Performance Analysis.....	5
Overspeed Control.....	6
Computer Analysis of Performance.....	7
Power Modulation at High Wind Speeds.....	8
Overspeed Control.....	9
Aerodynamic Starting.....	9
Power Increase at Low Wind Speeds.....	10
PRELIMINARY DESIGN.....	11
General.....	11
Airload Hinge Moment.....	12
Aileron Weight.....	13
Total Centrifugal Force on Aileron.....	14
Centrifugal Moment about Aileron Hingeline.....	14
Design of Centrifugal Force Drive System.....	16
Sizing Hydraulic Cylinders.....	16
Coordinating Aileron Deflection on the Two Blades.....	17
Aileron Twist.....	19
Aileron Latches.....	19
Design Summary.....	20
CONCLUSIONS.....	21
RECOMMENDATIONS.....	21
FIGURES.....	22
APPENDIX A - Modified Computer Code: PROP.....	31
APPENDIX B - Symbols.....	63
REFERENCES.....	65

LIST OF FIGURES

<u>Figure</u>	<u>page</u>
1 - Blade Planform Geometry-----	22
2 - Airfoil Section Characteristics with 20% Aileron-----	23
3 - Blade Element Velocities-----	26
4 - Effects of Aileron and Spoiler on Power Coefficient-----	27
5 - Effects of Aileron Control on Power at 33 R.P.M.-----	28
6 - Aileron Hardware-----	29
A-1 - Convergence Studies-----	57
A-2 - 20% Aileron Incremental Effects-----	58
A-3 - 10% Spoiler Incremental Effects-----	61

SUMMARY

Studies have been conducted to determine the feasibility of using aileron or spoiler controls as alternates to pitch control for large horizontal axis wind turbines. The NASA Mod-0 100 kw machine was used as the basis for this study. Specific performance studies were conducted for 20% chord ailerons over the outboard 30% span, and for 10% chord spoilers over the same portion of the span. Both control systems utilized control deflections up to 60°. Results of the study show that either ailerons or spoilers can provide the control necessary to limit turbine power in high wind conditions. The aileron system, as designed, provides overspeed protection at hurricane wind speeds, low wind speed starting torque of 778 N-m at 3.6 m/s, and a 1.3-1.5% increase in annual energy compared to a fixed pitch rotor. The aileron control system preliminary design study includes aileron loads analysis and the design of a failsafe flyweight actuator for overspeed protection in the event of a hydraulic system failure.

INTRODUCTION

Current large scale horizontal-axis wind turbines utilize variable pitch of all or a portion of blade span for starting, stopping, and modulation of speed. However, design of variable-pitch turbine blades of large size poses several structural and mechanical problems. Fixed-pitch rotors for large wind turbines offer advantages over variable pitch rotors or tip-controlled rotors. The blades of the fixed-pitch rotor are oriented so that the fatigue-producing cyclic gravity loads are in the direction of the greatest dimension (the section chordwise direction). This minimizing of cyclic stresses results in weight and cost savings. A fixed-pitch rotor does not require blade pitch bearings or the complex bearing assemblies and linkages needed for pitch control and further stress reduction results from combining a teetering hub with fixed pitch rotor. These factors contribute to significant cost savings of fixed-pitch rotors over variable-pitch rotors.

The fixed-pitch rotor, however, has two inherent problems: (1) start-up initiation and shutdown control, and (2) prevention of overspeed. Setting fixed-pitch blades at an angle to maximize annual energy may result in near-zero starting torques when the rotor axis is aligned with the wind, since the blades are completely stalled. It has been demonstrated that yaw control may be used for start-up of fixed-pitch wind turbines. However, yaw control is not fast enough to prevent overspeed. Yaw systems operate slowly; as much as one minute may be required to yaw sufficiently to prevent overspeed. Typical overspeed rates are so high that the rotor speed can double in half that time.

Although yaw control might be used to provide starting and to shut down at low wind speeds, other means are required for overspeed control. One possible concept is the use of retractable spoilers on the outboard portion of the blades to reduce rotor speed by decreasing section lift and by increasing drag. An alternative concept is the use of hinged trailing-edge surfaces (ailerons) which can act similarly to spoilers in preventing overspeed, and can also act to improve rotor torque at less-than-design wind speeds, thus improving annual energy output.

Spoiler and aileron control systems have been studied under a 6-month grant from NASA Lewis Research Center. This report presents results of these studies which include aerodynamic performance of aileron and spoiler controls and their effects on turbine performance, selection of a control system sized for the NASA MOD-0 38.1 m diameter wind turbine, and preliminary design of mechanical systems for control surface actuation and fail-safe operation.

PRELIMINARY CONSIDERATIONS

Control System Options Studied

Geometric variables available to the designer for the present study are: control surface type (aileron or spoiler), spanwise extent of control surface, control surface chord, and for the case of the spoiler, hingeline location. Most of the torque produced by a propeller-type wind turbine is produced by

the outer portion of the blade. For this reason, torque modulation devices should be located on this portion of the blade. The MOD-0 turbine uses pitch control over the outer 35% of the blade. Control surface span for aileron and spoiler studies was selected as the outer 30% (see figure 1).

Ailerons

Ailerons have several characteristics which make them attractive as candidates for wind turbine aerodynamic control. First, they produce nearly the same aerodynamic effects as spoilers of the same chord and deflection angle. Second, ailerons have the capability of providing positive as well as negative increments in lift. Furthermore, downward deflection of ailerons will increase maximum lift coefficient. The ability to increase lift at low wind speed conditions is attractive, since increased lift can be expected to result in increases in torque and hence power production.

Spoiler Type

Plate and plug type spoilers have both been successfully employed on aircraft (see sketch below).



Plate-Type Spoiler

Plug-Type Spoiler

Sketch A - Spoiler Types

The two types are essentially equal in terms of lift and drag increments produced for a given projection height. The plug type have low actuation loads, but reduce torsional stiffness and strength of the airfoil more than the plate type. The plate type also causes less penalty if mis-rigged, and they have hinge moments which tend to close them. Based upon these considerations, plate type spoilers were selected for the present application.

Spoiler Hingeline Location

Experiments have shown that spoiler effectiveness increases as the location of the spoilers is moved forward (ref. 1). Unfortunately, forward spoiler locations result in a time lag between actuation and change in lift. For this reason, forward spoiler locations have rarely been selected for airplane control systems. In the case of a wind turbine, time response requirements are not so severe. In aircraft, control response must occur within the time required to travel a few chord lengths. Low solidity wind turbines such as the MOD-0 machine have blade tips which travel a large number of chord lengths per

revolution (more than 100 chord lengths at mid-control position), and control response within one revolution is considered quite satisfactory. A second consideration for spoiler location is the effect on the structure of cutting into the airfoil, and a third consideration affecting the choice of spoiler type and location is the effect of "mis-trimmed" or "mis-rigged" spoilers on drag at conditions for which spoiler deflection should be zero. In addition, any gap or protuberance associated with the spoiler or actuating mechanism will add to the basic section drag, and the penalty associated with drag of this type is much more severe for forward locations than for aft positions. It is a cardinal rule of airfoil design that leading edges should be kept as smooth and uncluttered as possible. Based upon these considerations, the present design studies were conducted for spoilers with hingeline locations aft of 50% chord. Because of the availability of data for spoilers with a 70% hingeline, that location was selected.

PERFORMANCE ANALYSIS

Leading-Edge Suction Studies

Traditionally, aerodynamic characteristics of airfoil sections are studied in terms of lift and drag coefficient components of the resultant force. Another set of components, sometimes used, are normal and chordwise force coefficients. For a wind turbine blade element with zero twist and zero pitch, only the chordwise force produces torque. It is, therefore, instructive to study the airfoil characteristics in terms of this torque producing component, called "leading-edge suction." The relationships between c_l , c_d , and the chordwise and normal coefficients are:

$$c_s = c_l * \sin(\alpha) - c_d * \cos(\alpha) \quad (1)$$

$$c_n = c_l * \cos(\alpha) + c_d * \sin(\alpha) \quad (2)$$

where:

c_s = suction force coefficient, positive forward

c_n = normal force coefficient, positive upward

Figure 2 shows the c_l , c_d and c_s as functions of angle of attack for the NACA 23024 airfoil with 20% aileron. A theoretical relationship between c_s and angle can be derived for a symmetrical section from thin airfoil theory, as follows:

$$c_l = 2\pi\sin(\alpha), \quad c_d = 0 \quad (3)$$

Substituting these value relationships into equation (1) above, the following result is obtained:

$$c_s = 2\pi\sin^2(\alpha) \quad (4)$$

In real flow, drag is present, and at zero angle of attack c_s is equal to $-c_d$.

At angles of attack near stall, the suction decreases abruptly, and again becomes negative. Thus the useful angle of attack range for developing positive power is from the angle at which enough "theoretical" suction is developed to overcome the basic section drag, up to the angle of attack at which stalling occurs. For the NACA 23024 airfoil the range of angles for positive suction is between 2° and 17°. A second region of positive suction appears at about 60° and remains up to 90°.

The relationship between wind speed, rpm, and blade angle is shown in figure 3. When the turbine axis is aligned with the wind, the angle of attack on the blade will range from 90° at zero rpm to 0° at infinite rpm. For an untwisted blade element at zero pitch angle, the angle of attack will be equal to the angle ϕ . For low lift coefficients and low blade solidity, the induced velocity factors a and a' will be small. It is useful to assume the limiting case of zero induced effects to study trends. Setting $a = a' = 0$,

$$\tan(\alpha) = \tan(\phi) = \frac{V_{wind}}{\omega r} \quad (5)$$

Single Point Performance Analysis

Selecting the 75% radius station as a representative station for blade element analysis, this gives:

$$\tan \alpha = \frac{V_{wind}}{\omega (.75 R)} \quad (6)$$

Rearrange:

$$\omega = \frac{V_{wind}}{.75 R (\tan(\alpha))} \quad (7)$$

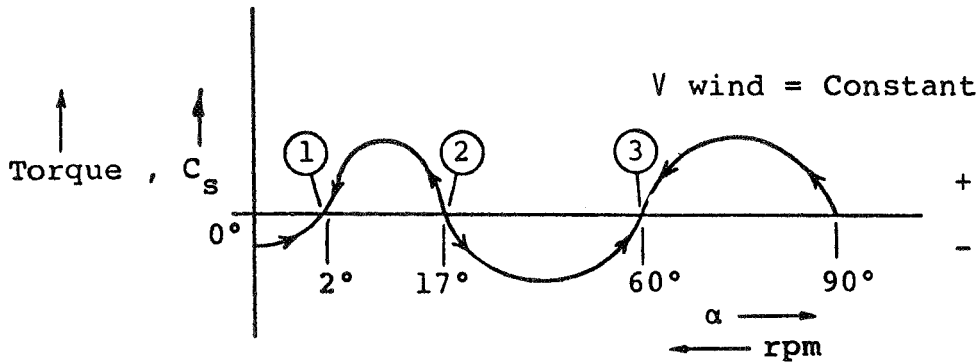
Using this relationship, and a specified wind speed, the rpm can be calculated corresponding to a given angle of attack. From the c_s curve for the NASA 23024 airfoil, it is seen that zero torque (zero c_s) will occur at several angles. For a wind speed of 54 m/s (120 mph), equilibrium rpm values are calculated as shown in Table 1:

Angle of Attack	Wind Speed	RPM
2°	54 m/s (120 mph)	1029
17°	54 m/s (120 mph)	116
60°	54 m/s (120 mph)	21

This study shows that the highest rotational speed corresponds to the lowest angle of attack.

The question of which of the possible equilibrium states will really exist is answered by considerations of stability. Examining the graph of c_s vs. α , and realizing that torque increases as c_s increases, and that rpm decreases as α increases, the question of stability is easily understood.

Sketch B shows these characteristics:



Sketch B - Stability

Since an increase in rpm from point 1 will result in negative torque, and a decrease in rpm will result in positive torque, it is clear that this point is in stable equilibrium. Point 2, on the other hand, has the opposite characteristics. An increase in rpm from point 2 will result in an increase in torque, accelerating the rotor toward point 1, and a decrease in rpm from point 2 will result in negative torque, decelerating the rotor toward point 3. Thus, point 2 is unstable. These same considerations will show that point 3 is a second stable equilibrium point.

These arguments are easily generalized to state that equilibrium points with positive slope on the graph illustrated will be stable, while equilibrium points with negative slope will be unstable. To protect the wind turbine from overspeeding in high wind with loss of electrical load on the generator, it is necessary that either no stable equilibrium states exist, or that the stable equilibrium "runaway" rpm be low enough that no damage will be sustained, and the remaining rotor energy can be absorbed by the system mechanical brake. Sketch B shows that point 1 is the most dangerous equilibrium point, since it corresponds to the highest stable equilibrium rpm.

Overspeed Control

In the event of electrical failure of a generator being powered by a wind turbine, it is necessary to provide means for preventing overspeed or "runaway" which would result in overstressing of the rotor structure and subsequent failure. For large wind turbines this poses a difficult problem for a mechanical brake design. The preferred method is to use aerodynamic braking such as pitch control or similar means. The braking device must be capable of functioning not only at the rated or design wind speed, but also at the highest wind likely to be encountered. For the present study a hurricane wind speed of 54 m/s

(120 mph) was selected as the maximum wind speed. Combining the requirements of a "double emergency" situation consisting of generator failure along with hurricane wind results in a design requirement to prevent overspeed with zero torque and wind velocity of 54 m/s.

Figure 2 shows the relationship of c_s and angle of attack for aileron deflection of -60° , and spoiler deflection of 60° . The results for 60° upward deflection of either spoiler or aileron show that the region of positive c_s in the low (pre-stall) angle of attack range has been eliminated. Thus, no positive torque will be developed over this range of angles. At angles of attack beyond 60° however, positive c_s persists even with aileron or spoiler control surface deflected upward 60° , and positive torque will be developed. From the arguments given earlier, an equilibrium "runaway" state can be expected at conditions corresponding to 60° angle of attack. For the hurricane wind speed of 54 m/s, the equilibrium rotational speed will be about 21 rpm. Since this rotational speed is well below the operating speed of 33 rpm, it does not pose a hazard in terms of centrifugal blade loads. Mechanical braking must be used to bring the rotor to rest.

From these preliminary studies based upon simplified analysis and hand calculations, it is indicated that either a spoiler or an aileron system will be adequate for providing overspeed protection to the turbine. The next section documents more sophisticated computer studies of turbine performance with aileron and spoiler controls, which confirm these preliminary findings.

Computer Analysis of Performance

Analysis of performance of the MOD-0 wind turbine was conducted using the PROP computer code (see ref. 2), modified as explained in Appendix A. The program receives input information about rotor geometry, control mode (tip section pitch, spoilers, or ailerons), and operation (varying rpm or wind speed) through a series of data cards. For the analysis reported here, the following input items were considered constant and were not varied:

B = 2	(number of blades)
BO = .97	(NASA tip loss model)
XETA = 0.167	(velocity power law exponent)
HB = 2 ft	(hub radius)
R = 62.5 ft	(turbine radius)
THETP = 0 deg	(pitch angle)
THETI = 0 deg	(twist angle at all inboard stations)
H = 100 ft	(hub altitude)
SI = 0 deg	(coning angle)

Blade planform geometry used in all calculations corresponds to the wooden inboard blade (shown in figure 1). The length of the spoilers and ailerons is 30% of radius. This geometry was entered by means of data cards.

Input data which were varied during this study included:

V	freestream wind velocity
OMEGA	angular velocity of turbine rotor
MCON	method of control (tip section pitch, spoilers, or ailerons)
TIPICH	angle of pitch of tip section
AILDEF	angle of deflection of ailerons
SPDEFL	angle of deflection of spoilers

The program permits use of various sizes of radial increments in the calculation of performance. Early in the analysis studies, comparison was made of results of computation using radial steps ranging from 10% to 2%. To minimize error, 2% increments were used in all subsequent calculations.

In operation, the computer program starts at the outboard end of the blades and calculates components of forces for each incremental radial blade element, working inboard to the hub.

Local chords and amount of twist are determined by the subroutine SEARCH using linear interpolation. Subroutine CALC is then called to calculate axial and rotational interference factors (a and a'), local angle of attack and lift and drag coefficients. Relative wind relationship to the blade section is shown in figure 3. The relationships between angle of attack and lift and drag coefficients of the NACA 23024 airfoil are obtained from subroutine NACAXX and modified by subroutines TIPLOS (tip and hub losses) and INCREM (increments of c_{ℓ} and c_d due to aileron or spoiler deployment).

As can be seen in figure 3, angle of attack is a function of a , and a is a function of the section lift. Thus, evaluation of a is an iterative process which is discussed in detail in Appendix A. The program may be controlled to limit a between -0.5 and $+0.5$, or to set $a=0$, or to permit a to be unlimited. Following computer runs to study the effectiveness of these schemes, remaining performance predictions were calculated with the restriction that $-0.5 \leq a \leq 0.5$. Radial interference (a') was assumed zero for all the present studies. Local elements of force in the plane of rotation (producing torque) and normal to the rotor plane (producing thrust) are determined by iteration at both ends and at the center of each blade section, and the forces are integrated across the blade to give total quantities for the blades. Details of the airfoil aileron, and spoiler modeling are given in Appendix A.

Power Modulation at High Wind Speeds

For wind speeds greater than the wind speed for which the electrical generator is rated, it is necessary to either take the wind turbine off-line or to "dump" power by aerodynamic or other means. With an aileron or spoiler control system this "dumping" is accomplished by deflecting the control upward to reduce lift and torque. Figure 4 shows power coefficient versus tip speed ratio for the basic rotor, and the rotor with full up aileron, and with full up

spoiler. These results also show that either the aileron or spoiler can provide the control necessary to reduce power to zero over the normal range of tip speed ratios. Because of the potential of the aileron to provide starting torque and to provide increased power at low wind speeds, the aileron was selected for further studies.

The data in figure 4 show that the aileron chord could be reduced considerably, perhaps as much as 50%, and still provide necessary overspeed protection. While smaller aileron chord would reduce cost, it was decided to retain the 20% aileron chord size for two reasons. First, if one aileron became inoperative the rotor could be stopped with the remaining aileron. Second, it is known from experimental tests that the PROP code and similar theoretical methods under-predict maximum power by a considerable amount. Therefore, a substantial margin must be provided in the design of a control system using these analytical methods. If experimental evaluation of the new control system reveals that it is oversized, corrective action can be taken at that time. Improved aerodynamic modeling for wind turbines should be developed to reduce discrepancies between theory and experiment in order to reduce costs of experiments and avoid expensive design errors.

Figure 5 shows how power modulation would be accomplished with the 20% aileron control system for a synchronous generator operating at 33 rpm. For wind speeds lower than 8.2 m/s (18 mph) with zero control deflection, the power developed is lower than the rated value of 120 kW shaft power, corresponding to 100 kW of electrical power. For wind speeds in excess of 8.2 m/s (18 mph), the turbine is capable of producing more power than the generator can absorb. By deflecting the control surface upward, power can be modulated to provide the required 120 kW at speeds up to 12.9 m/s (29 mph). For speeds greater than this value, it will be possible to provide 120 kW by using down aileron deflection, an option not possible with spoilers. Thus the aileron system can provide rated power up to 15.6 m/s (35 mph).

Overspeed Control

Computer studies with full up aileron were conducted at the hurricane wind speed (54 m/s) condition described earlier, for rotational speeds ranging from 10 to 30 rpm. These runs show that the zero torque "runaway condition" occurs at 19 rpm. This value compares very favorably with estimate of 21 rpm from the simplified analysis given in Table 1, and confirms that the proposed control system will provide adequate overspeed protection.

The control system must be capable of providing actuation forces sufficient to overcome the closing aerodynamic hinge moment. The critical design condition is maximum overspeed rotational speed of 40 rpm with 60° up aileron at zero wind speed. The hinge moment for this case is 186 N-m per aileron.

Aerodynamic Starting

Wind turbines with pitch control are ordinarily started by rotating the blades to an unstalled angle, and then decreasing the pitch angle as rpm

increases. With a fixed pitch rotor, very little starting torque is developed, and other means for starting must be employed.

Recent tests by NASA with the MOD-0 turbine have demonstrated that starting can be effected in a fixed pitch mode by yawing the rotor away from the wind. While this mode of operation is possible for a large scale machine, it is inconvenient in that yaw rates must be low to prevent over-stressing the rotor system.

With an aileron control system it is possible to generate starting torque without yawing the rotor away from the wind. At zero rpm the effective angle of attack is 90° , which means that the basic blade will be fully stalled, and torque will be nearly zero. With up aileron, however, a larger starting torque is provided. The computer code used for performance studies is not capable of calculation at zero rpm, so runs were made at very low rpm values, and the results were extrapolated to zero rpm. This study shows that the optimum aileron angle for starting is -60° , and that a starting torque of 778 N-m (574 ft-lb) is available at a wind speed of 3.6 m/s (8 mph). Because of the dynamic pressure effect, this torque will be proportional to the square of the wind speed. Table 2 shows starting torque for several wind speeds.

Whether starting by use of ailerons can actually be effected depends upon two factors which have not yet been determined. First, the friction of the generator and gear train must be overcome. Second, once starting is achieved, rpm must be increased to the point that the blades become unstalled so that the operating speed of 33 rpm can be achieved. Accelerating the rotor to an unstalled state cannot be simulated with the present computer codes. Full-scale rotor tests will be required to evaluate the practicality of this starting method.

Table 2 - Starting Torque with 60° Up Aileron

<u>Wind Speed</u>	<u>Torque</u>
2.2 m/s (5 mph)	304 N-m
3.6 m/s (8 mph)	778 N-m
4.5 m/s (10 mph)	1216 N-m

Power Increase at Low Wind Speeds

Another interesting control option is possible with the aileron system. At wind speeds lower than rated, positive aileron deflection can be utilized to increase power available.

In order to assess the benefits of aileron deflection at speeds below rated, it is necessary to calculate annual energy output for competitive control

schemes using some mathematical model for the wind probability distribution. In the present study, a Rayleigh distribution has been used. Table 3 shows results of a study of this type, comparing zero control with optimum aileron deflections. Optimum aileron deflections are 5° or lower.

Table 3 - Use of Ailerons to Increase Annual Energy

	Mean Wind Speed		
	5.36 m/s (12 mph)	5.81 m/s (13 mph)	6.26 m/s (14 mph)
Increase in Annual Energy	1.8%	1.6%	1.3%

These results show that using optimum aileron provides small gains in annual energy. If the rated power were higher, or mean wind speeds lower, larger increases would result.

PRELIMINARY DESIGN

General

The general configuration of the aileron control system (shown in figure 6) was selected based upon airplane flight control design experience, two-dimensional wind tunnel research of aileron and spoiler control systems, and performance studies of the MOD-0 wind turbine using the PROP computer program, with the airfoil subroutine modified to accommodate aileron control characteristics. From these latter studies, it was determined that an aileron of 20% chord and 60° upward deflection having a span extending over the outer 30% of the rotor would provide adequate overspeed protection. The 15° down travel is adequate for providing added power at low wind speed conditions. A bell crank transfers spanwise motion of a primary push rod to chordwise motion. The primary push rod is actuated by a hydraulic cylinder located in the inboard portion of the rotor.

The counter-weight shown in the figure acts under the influence of centrifugal force to drive the aileron to the full up position, providing fail-safe operation in the event of hydraulic system failure. The hydraulic cylinder works against the weight to bring the aileron to a desired setting. The decision to locate the hydraulic cylinder on the rotating blade was made largely because of existing hydraulic hardware used for pitch control on the MOD-0 machine. In other applications it would be quite feasible to locate the hydraulic cylinder within the rotor hub, and transfer the needed spanwise actuator motion through a push rod extending to the rotor hub. A mechanical latch locks the ailerons in the full up position until released by restoration of hydraulic system pressure.

It is desirable to locate the aileron hingeline near the airfoil upper surface rather than on the mean line for two reasons. First, when deflections of as much as 60° are to be used, the airfoil surface forward of the aileron must be cut back to a position well forward of the hingeline to clear the deflected aileron. This clearance produces a large gap in the airfoil surface when the aileron is in neutral position; this gap is an added source of drag. Moving the hinge toward the upper surface minimizes the gap size and the drag. Second, upper surface hinging permits maximum moment arm inside the airfoil contour for attachment of the aileron actuating mechanism.

On a straight-tapered blade of constant percentage thickness most parameters that need to be calculated can be stated in terms of local blade chord which, in turn, depends upon blade station (radial distance from the center of rotation).

The Dimensional quantities given in this section of the report are in English units rather than S.I. units because of current fabrication practice. In the calculations which follow, two aileron planform arrangements are considered. For one planform the aileron extends from the 69.1% radius (518.34 in. station) to the rotor tip, and for the second case the aileron extends from 64.7% radius (485.00 in. station) to the rotor tip. Performance studies show that either arrangement will be satisfactory. The present design loads analysis will also indicate that no critical loading situation will occur for either geometric arrangement. For the present planform geometry, local blade chord is given by:

$$c = 7.05786 - .0867925 x \quad (8)$$

where c = local chord, ft
 x = local radial distance, ft

Airload Hinge Moment

Data from several sources indicate that the maximum value of closing hinge moment coefficient, c_h , that can be expected with the aileron deflected up (downwind) 60° will be less than 0.58. To be conservative, a value of 0.58 will be used for the present design study.

Maximum hinge moment will occur when the angle of attack of the blade is nearly 0°, i.e., when rotational velocity is high and wind velocity is low. In this case, resultant velocity on the blade outboard sections will come almost entirely from rotational velocity and can be taken as $v = x\omega$. A rotational velocity of 40 rpm (4.189 radians/sec) will be used for design.

Measured along the upper surface from the hingeline to the trailing edge, the aileron chord is .1930 of the local chord c . Thus, at any blade station, the incremental airload hinge moment will be

$$H = \int c_h q c_a^2 dx \quad (9)$$

where H = hinge moment

$$q = \frac{1}{2} \rho (\omega x)^2$$

$$c_a = .193c$$

and c is given by equation (8).

Using sea-level standard air density and 40 rpm, the following results are obtained:

<u>H</u>	<u>Inboard Aileron Station</u>
2412 in-lb	518.34 in
2808 in-lb	485.00 in

Aileron Weight

The flat-pattern area of sheet metal required to make the aileron skin at any station is approximately $.5557c$ per unit span. Total skin weight is calculated by integrating across the span of the aileron:

$$w_s = \int w * t * \frac{dA_s}{dx} * dx \quad (10)$$

where w = specific weight of aluminum, 0.10 lb/in^3

t = skin thickness, $.020 \text{ in}$

$\frac{dA_s}{dx}$ = skin area per unit span = $.557c$

c = a linear function of x , from equation (8)

The sheet metal area required for a rib at any station is approximately $.765c$ for flanges plus $.01240c^2$ for the rib web. Treating ribs as distributed weight, rib weight equals

$$w_r = \int w * t * \frac{dA_r}{dx} * dx \quad (11)$$

where $\frac{dA_r}{dx}$ = rib area per unit span - rib area/rib spacing

$\frac{dA_r}{dr} = (.765c + .0120c^2)/\text{rib spacing}$

(The rib spacing in this case is 10 inches.)

Hinge and trailing edge strip will contribute about .027 lb/in. Rivets, etc., are estimated to weigh about 1.0 lb total. The total weight of one aileron is given by:

$$W_{total} = W_{skin} + W_{ribs} + W_{hinge+TE} + W_{rivets} \quad (12)$$

<u>Total Weight</u>	<u>Inboard Aileron Station</u>
17.8 lb	518.34 in
21.0 lb	485.00 in

Total Centrifugal Force on Aileron

The total centrifugal force on the aileron is obtained by a span-wise integration:

$$F_c = \int \omega^2 \times \frac{dm}{dx} dx \quad (13)$$

where $\frac{dm}{dx}$ = mass per unit span - weight per unit span/g

Using the weight equations developed earlier for various components of the aileron, and assuming "distributed" rib mass as earlier, the following result is obtained for $\omega = 40$ rpm.

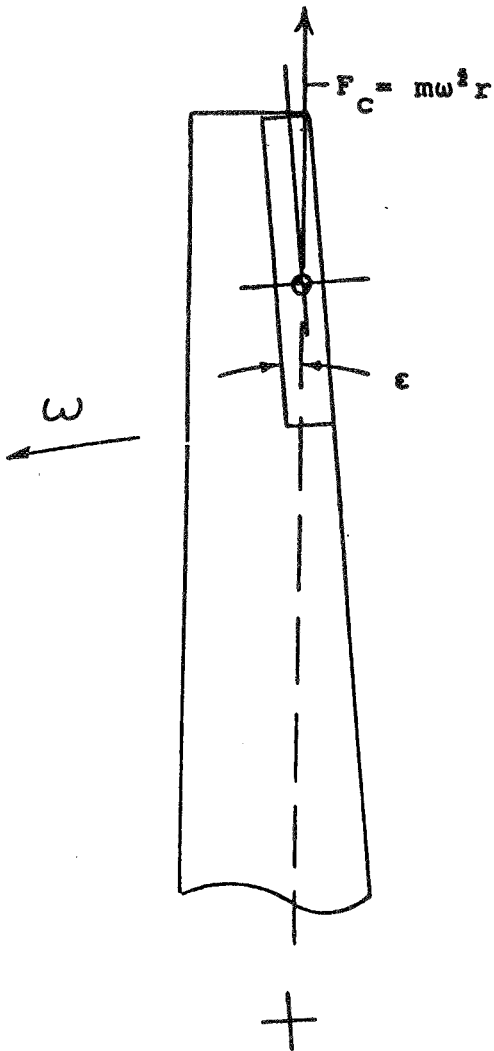
<u>Centrifugal Force</u>	<u>Inboard Aileron Station</u>
511 lb	518.34 in
582 lb	485.00 in

Centrifugal Moment about Aileron Hinge Line

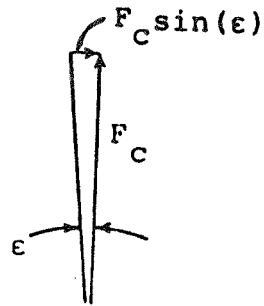
Since centrifugal forces on incremental mass elements of the aileron act neither through, nor parallel to, the aileron hinge line, these forces produce moments about the hinge line as shown in Sketch C on the following page.

The hinge moment at any station is the local centrifugal force times the sine of the angle between the hinge line and a true radius, multiplied by a moment arm equal to the perpendicular distance between the hinge line and the line of action of the centrifugal force through the local section c.g. The magnitude of these moments are calculated below. Hinge mass is neglected since the moment arm is so short.

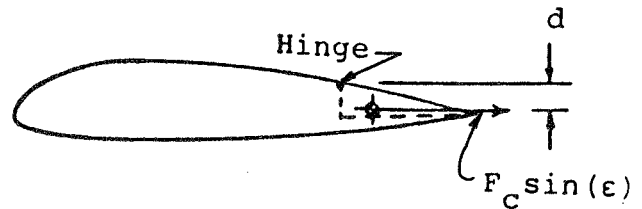
For ribs, skin and trailing edge strip, the c.g. can be taken as being .053c below (upwind of) the hinge line. This is the dimension "d" in Sketch C. The direction of the hinge line, relative to the center-line of the steel tube



(a) Rotor and Centrifugal Force



(b) Chordwise Centrifugal Force



(c) Hinge offset

Sketch C - Centrifugal Moment

spar of the blade is .05066 radians. The direction of the centrifugal force at the c.g. of any aileron section relative to the spar center-line is approximately .6152 (c/r) radians. Thus $\epsilon = .05066 + .6152(c/r)$ radians.

Multiplying the force component by its moment arm about the hinge line and integrating over the aileron span gives:

$$H_C = \int (\omega^2)(x)(\sin \epsilon)(d) \frac{dm}{dx} dx \quad (14)$$

ϵ is a small angle, so $\epsilon \approx \sin \epsilon$.

Substituting all values and integrating, the following results are obtained:

<u>Centrifugal Hinge Moment</u>	<u>Inboard Aileron Station</u>
68.4 in-lb	518.34 in
75.2 in-lb	485.00 in

These values are much lower than the aerodynamic hinge moment.

Design of Centrifugal Force Drive System

Maximum airload hinge moment to be overcome = 2808 in-lb. To assure excess capacity to drive the aileron to full up position, design for $2808 \times 1.5 = 4212$ in-lb moment. The centrifugal moment produced by the aileron mass will be neglected for conservatism in this analysis.

Push rod moment arm about hinge line at full up aileron = 3.05 in. Thus push rod load = $4212/3.05 = 1321$ lbs. Push rod moment arm about bell crank pivot is also 3.05 in.

Counter-balance mass c.g. has a moment arm of approximately 11 inches when aileron is 60° up. Thus, the centrifugal force needed to supply 4212 in-lb moment is $4212/11 = \underline{383}$ lbs.

The mass is located at $x = 510$ in. Therefore the centrifugal load factor at 40 rpm (4.189 rad/sec) will be:

$$n = \frac{x\omega^2}{g} \quad (15)$$

Substituting,

$$n = 23.18$$

the weight required will be

$$w = \frac{F}{n}$$

$$\underline{w = 16.52 \text{ lb}}$$

Thus a centrifugal weight of this size will be able to overcome the aerodynamic hinge moment at 40 rpm and 60° up aileron with a 50% margin of safety, and taking no credit for the centrifugal effect of the aileron mass.

Sizing Hydraulic Cylinders

Moment arm of the actuating cylinder force to oppose the centrifugal force will be approximately 3.9 inches with aileron up 60° . Assuming (in the extreme)

that ω is still 40 rpm and airload hinge moment has fallen to zero, the actuating cylinder load required to start the aileron down will be $(4212/3.9) = \underline{1080 \text{ lbs.}}$

If it is desired to produce this force with hydraulic pressure of 1000 psi or less, net effective piston area of the activating cylinder needs to be:

$$A = \frac{F}{p} \quad (16)$$

$$\underline{A = 1.08 \text{ in}^2}$$

Assuming a piston rod diameter of 0.50 in, a piston diameter of 1.375 in will be more than adequate.

Total piston travel available should be 5.5 in. The fluid volume change associated with full travel will be:

$$\text{Vol} = \frac{\pi}{4} (D_o^2 - D_i^2)(L) \quad (17)$$

$$\underline{\text{Vol} = 7.1 \text{ in}^3}$$

Coordinating Aileron Deflection on the Two Blades

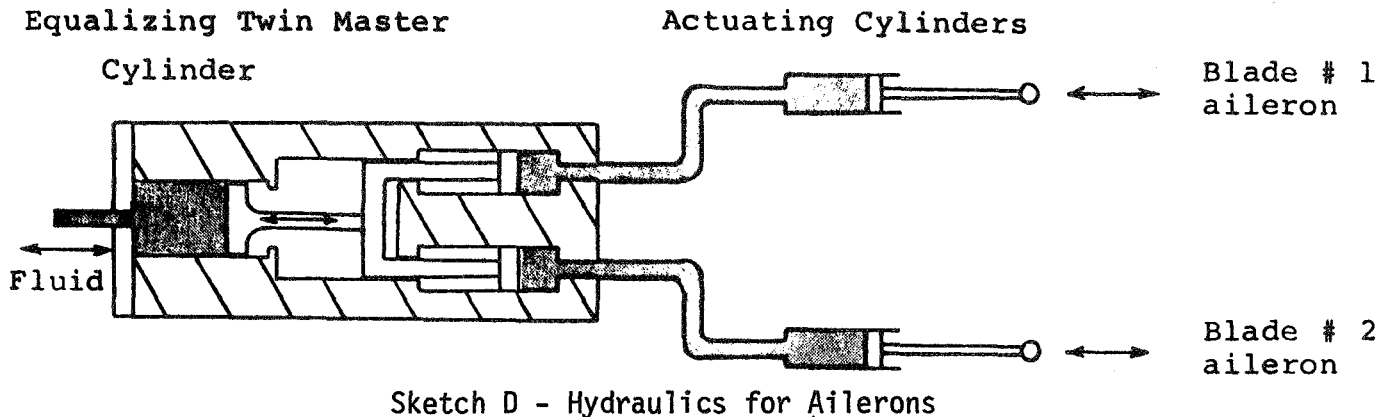
Because of physical constraints imposed by the configuration of existing MOD-0 rotor design, it is desirable that position coordination between the ailerons on the two blades be accomplished hydraulically rather than by mechanical interconnect between the two ailerons as originally proposed. Assuming identical actuating cylinders and aileron drive linkages in the two blades, this requires some means of guaranteeing equal fluid volume flows to or from the two actuating cylinders as aileron position is changed.

Since it is unlikely that loads in the two linkages will always be the same even though aileron positions may be the same, maintaining equal pressures in the two actuating cylinders will not satisfy the equal volume change requirement. Thus, merely splitting the flow from one pressure source will not do.

One simple way to guarantee equal volumes is to use some such arrangement as that shown on Sketch D on the following page. This arrangement provides a closed hydraulic system for each blade. Two identical master cylinders (shown as two chambers in a single housing) are driven by a single primary actuator. The two master cylinders and the cylinder that drives them constitute the unit labeled "motion equalizer assembly" on the drawing.

Except for the effects of leakage, such an arrangement will keep positions of the two slave cylinders coordinated even though pressures in the two systems are different. Since no hydraulic system can be absolutely leak-free, it seems advisable to provide a means of supplying makeup fluid to each of the two closed systems to compensate for small amounts of leakage. Such a system would

require position sensors on each of the slave cylinders and on the motion equalizer assembly. When either slave cylinder position does not agree with equalizer unit position within acceptable limits, an injector (perhaps solenoid actuator) would inject a small amount of fluid into that system. It is emphasized that the proposed arrangement would compensate only for very low leakage rates. Any gross leak would result in shutdown for repairs.



All of the items described above could be mounted on the rotor. If this were done and the primary hydraulic supply were mounted on non-rotating structure, one fluid transfer gland on the rotor shaft and slip rings to supply power for the injector systems would be required in addition to whatever slip rings were needed for instrumentation and control circuits.

The primary supply system could also be rotor-mounted thus eliminating all fluid transfer glands. However, the number of slip rings probably would be considerably increased if this were done. It appears that means could be provided to mount both the motion equalizer package and the pressure supply package on the outside surface of the rotor hub. At 40 rpm and a radius of 2.0 ft, centrifugal loads will be only 1.1 g. It should be possible to mount all required hardware well within a 2.0 ft radius.

Irrespective of where the components are located, the hydraulic cylinders will be sized as follows. The full area of the pistons in the twin master cylinder will be available. Thus the diameter will be:

$$D = \sqrt{\frac{4}{\pi} A} \quad (16)$$

where $A = 1.08 \text{ in}^2$.

Thus

$$D = \underline{1.17 \text{ in}}$$

Pressure in the single cylinder driving the twin master cylinders will be essentially the same as in each of the two driven cylinders if the single cylinder is made 1.75 inches in diameter. Its total volume flow requirement would be $5.5 \times 1.75^2 \pi/4 = 13.23 \text{ in}^3$.

To allow the ailerons to move quickly from normal operating position to full up-position for emergency shutdown of the wind turbine, the line(s) from the dump valve to reservoir must be designed to allow a high flow rate at low pressure.

Aileron Twist

Since the aileron actuation will take place at the inboard station, and the aerodynamic hinge moment is distributed along the span, the aileron will be subjected to torsional loading. The deflection in torsion (twist) is calculated by analyzing the aileron as a thin-walled cylinder (non-circular). The appropriate equation (from ref. 7) is:

$$\theta = \int \frac{T\ell}{4A^2Gt} dx \quad (17)$$

where T = applied torque per unit span
 ℓ = perimeter of thin-walled member (aileron)
 A = cross-sectional area of aileron
 G = elastic modulus in shear of aluminum (3.8×10^6 psi)
 t = skin thickness (.020 in)

T, ℓ , and A are all functions of local chord, which in turn depends on x. This analysis ignores rib and hinge contributions to torsional stiffness. The design condition is again the case of 40 rpm with 60° up aileron. The results of this analysis are given below:

<u>Total Twist</u>	<u>Aileron Inboard Station</u>
3.30°	518.34 in
3.88°	485.00 in

This amount of twist is considered to be quite acceptable.

Aileron Latching

A spring-loaded latching system is proposed to hold the ailerons in full up position once they have been fully deflected. Hydraulic pressure would work against the spring for the subsequent re-start. This could be accomplished by providing for over-travel where the actuator cylinder is attached to the centrifugal mass arm so that initial piston motion when hydraulic pressure is re-applied will release the latch and further motion will bring the aileron toward the neutral position.

On sudden loss of electrical load, a dump valve in the pressure supply system would be opened. Overspeed and/or manual shutdown signals also would be fed into the control for this valve. The same signals would be used to interrupt power to the pump drive motor.

Design Summary

The design information is summarized as follows:

Aileron Material: .020 in thick 2024T4 aluminum
(ribs and skin)

	<u>Aileron Inboard Station</u>	
	<u>518.34 in</u>	<u>458.00 in</u>
Aileron Weight: (each)	17.8 lb	21.0 lb
Centrifugal Force: (radial)	511 lb	582 lb
Centrifugal Hinge Moment: (opening)	68 in-lb	74 in-lb
Aerodynamic Hinge Moment: (closing)	2412 in-lb	2808 in-lb
Aileron Twist Under Maximum Moment:	3.3°	3.9°
Centrifugal Weight:	16.5 lb	19.2 lb
<u>Hydraulics (1000 psi system)</u>		
<u>Actuating Cylinder</u>		
Actuator Force:	1080 lb	1257 lb
Piston Diameter: (w/0.5 in. D. shaft)	1.375 in*	1.375 in
Travel (minimum):	5.5 in	5.5 in
<u>Flow Equalizer</u>		
Twin Piston Diameters:	1.17 in	1.17 in
Driving Piston Diameter:	1.75 in	1.75 in

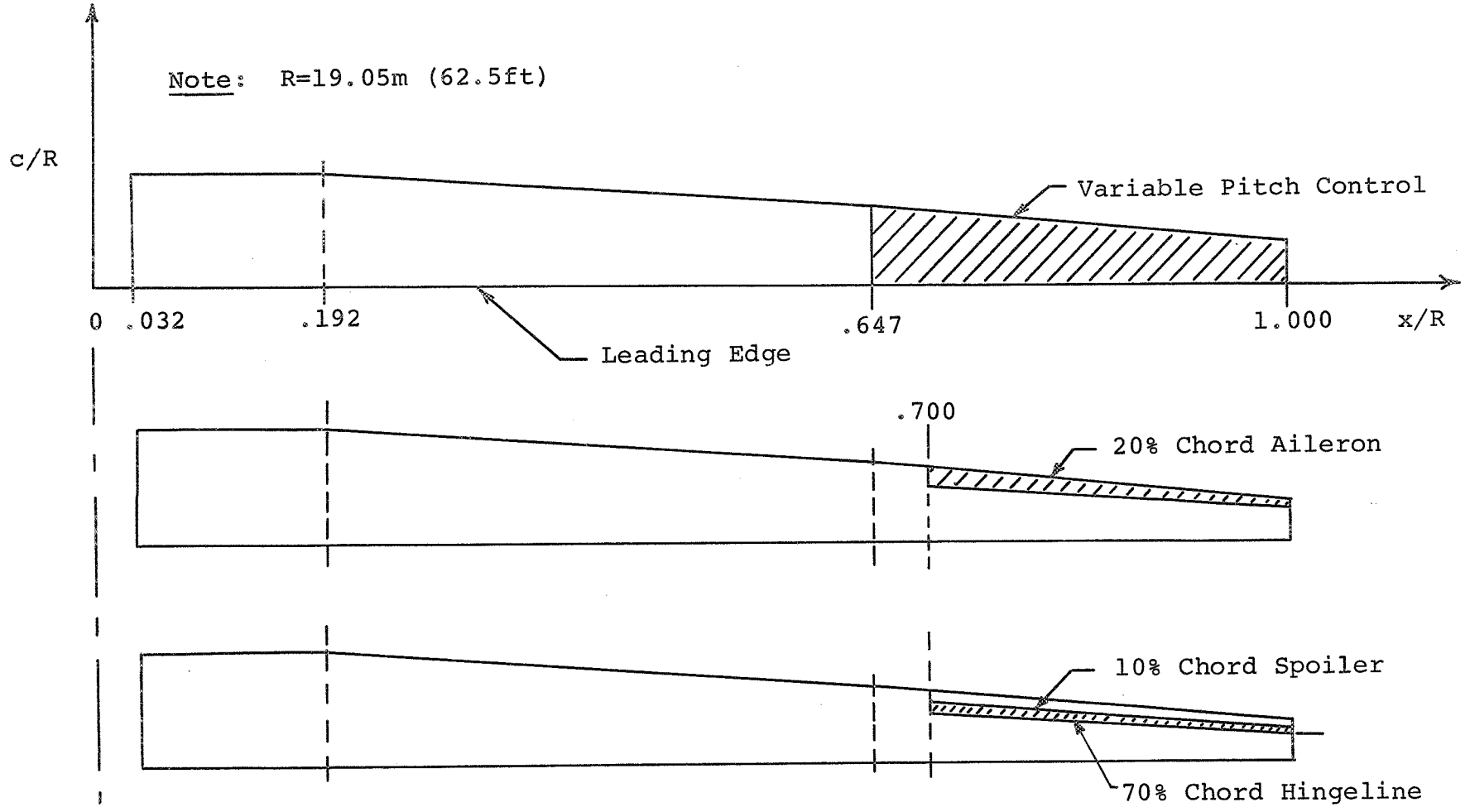
*This cylinder is slightly oversized to be a standard dimension.

CONCLUSIONS

1. Either ailerons or spoilers could be used to prevent runaway and to modulate power at higher than rated wind speeds.
2. An aileron system was selected as prime candidate for the present application, based upon considerations of providing power output gains at low wind speeds, and the possibility of starting without yawing the rotor away from the wind.
3. Preliminary loads analysis including hinge moments have been developed for a 20% chord, 30% span aileron control system for the MOD-0 turbine.
4. The system, as designed, provides overspeed protection at hurricane wind speeds, low wind speed starting torque of 778 N-m at 3.6 m/s, and 1.3 to 1.5% increase in annual energy compared to a fixed-pitch rotor.

RECOMMENDATIONS

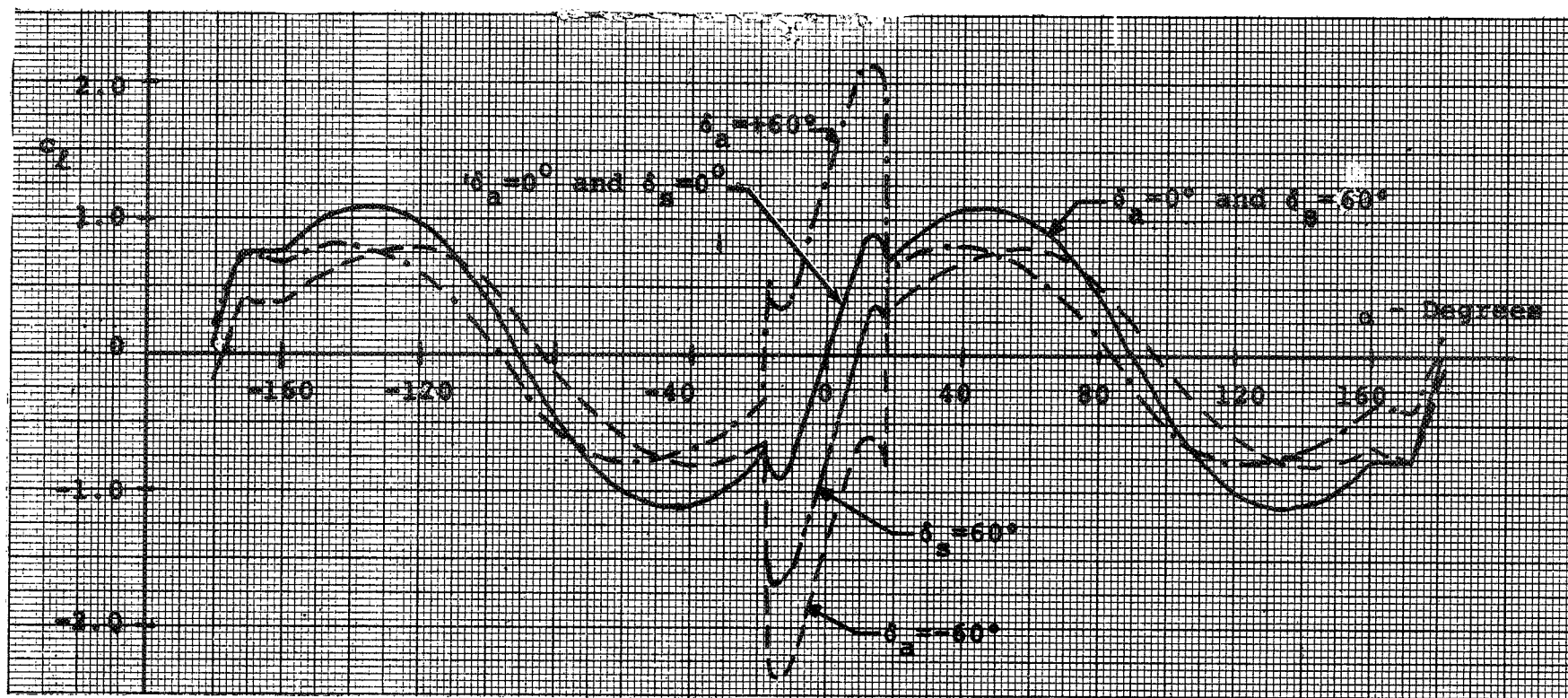
1. Aileron hardware should be developed for testing the aileron control concept on the MOD-0 turbine.
2. Theoretical models for wind turbine performance should be improved to diminish the disparity between theoretical and experimental power values.
3. Wind tunnel tests should be conducted to provide a better data base for airfoil characteristics at high (up to 90°) angle of attack, with and without control surface deployed.



Chord Lengths	
x/R	c/R
.032	1.0960
.192	1.0960
.647	.0640
1.000	.0333

Figure 1 - Blade Planform Geometry

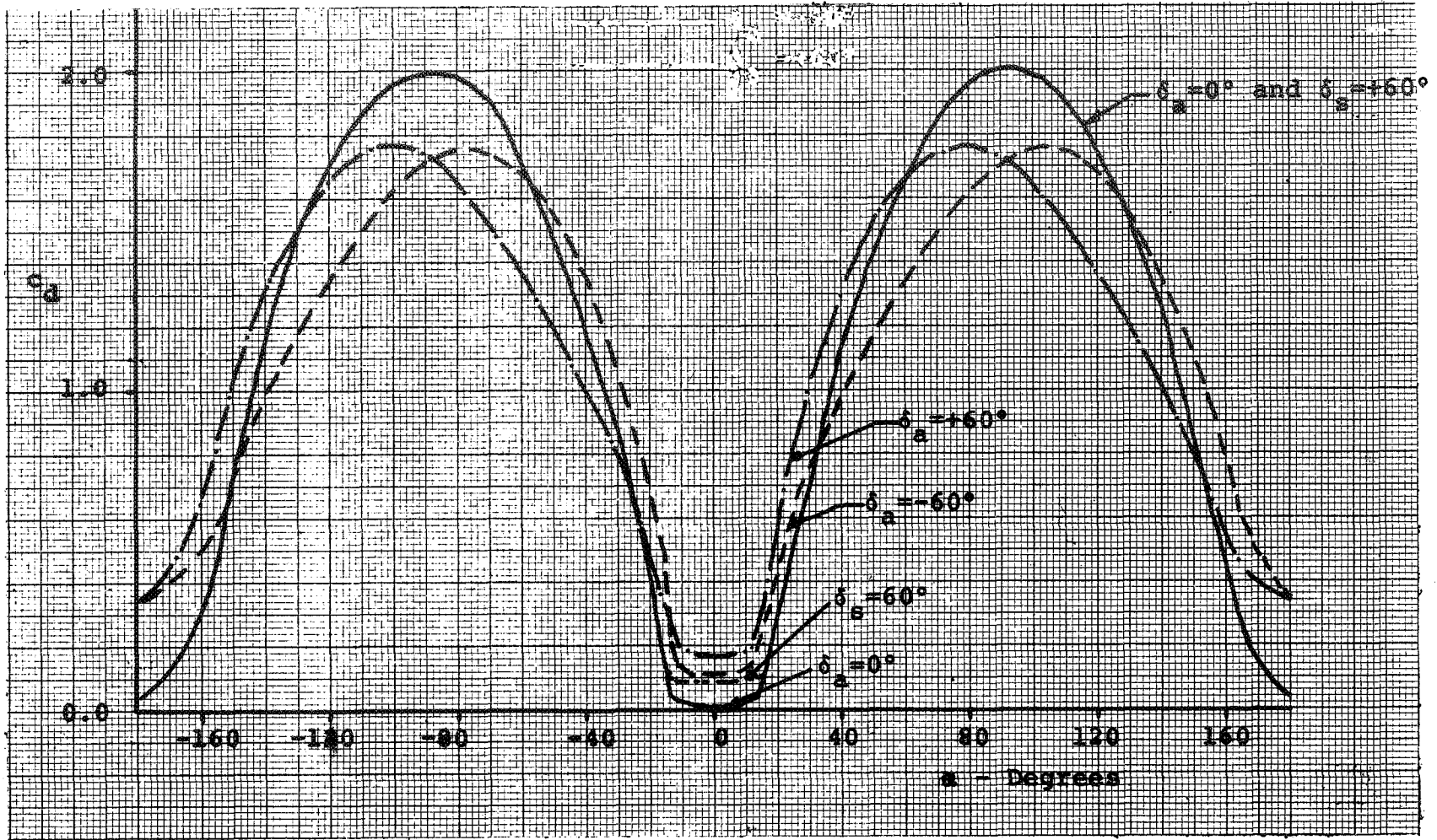
Note: Spoiler has no effect on lift for $|\alpha| > 17^\circ$.



23

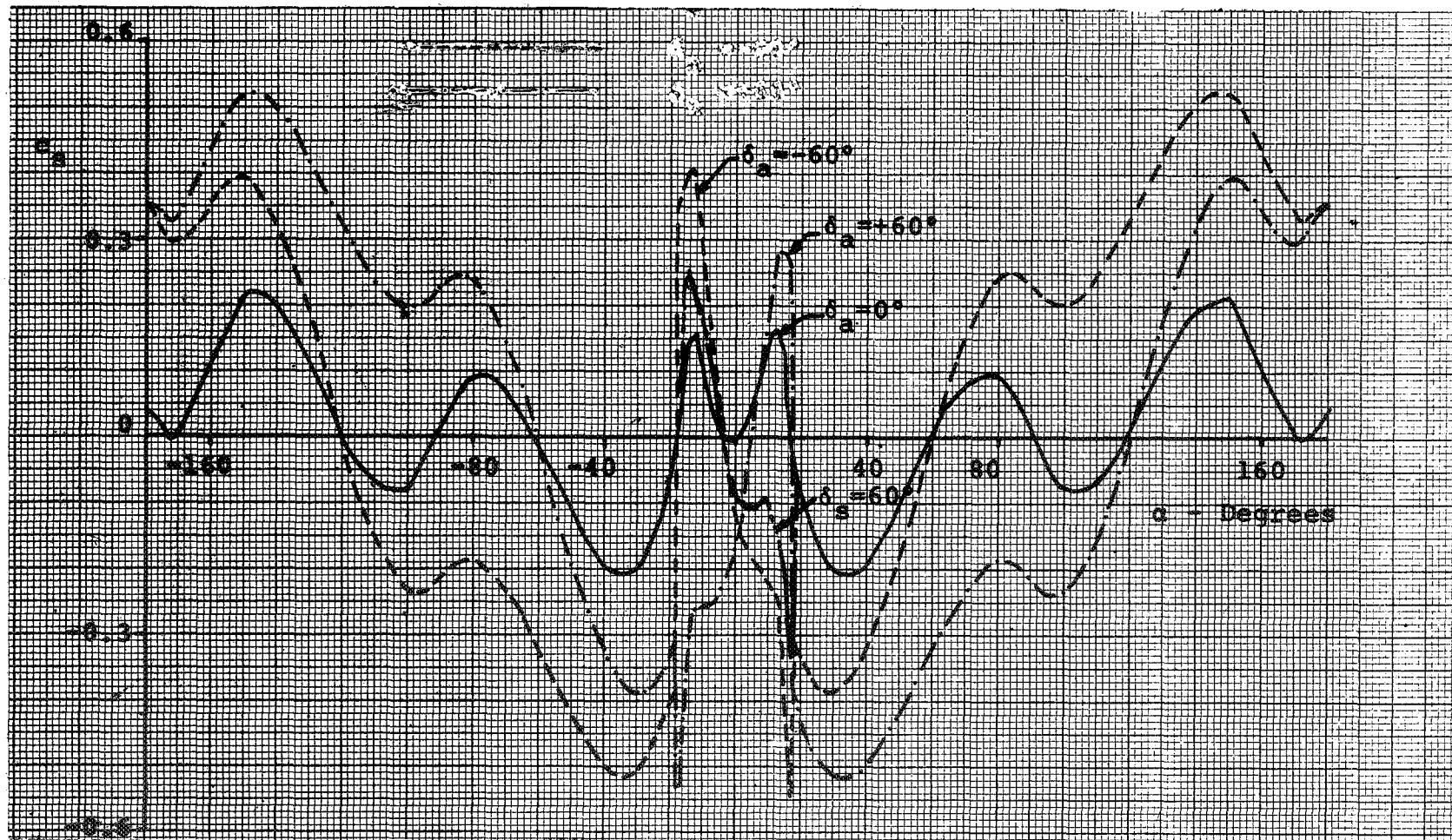
(a) Lift

Figure 2 - Airfoil Section Characteristics with 20% Aileron and 10% Spoiler.



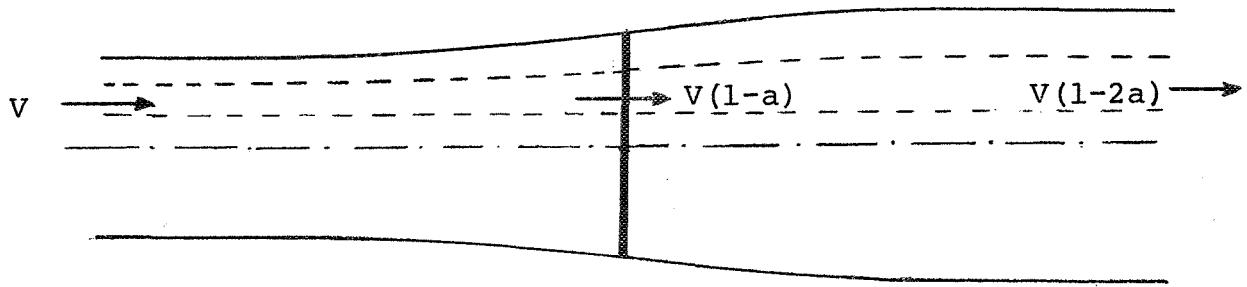
(b) Drag

Figure 2 - Continued.

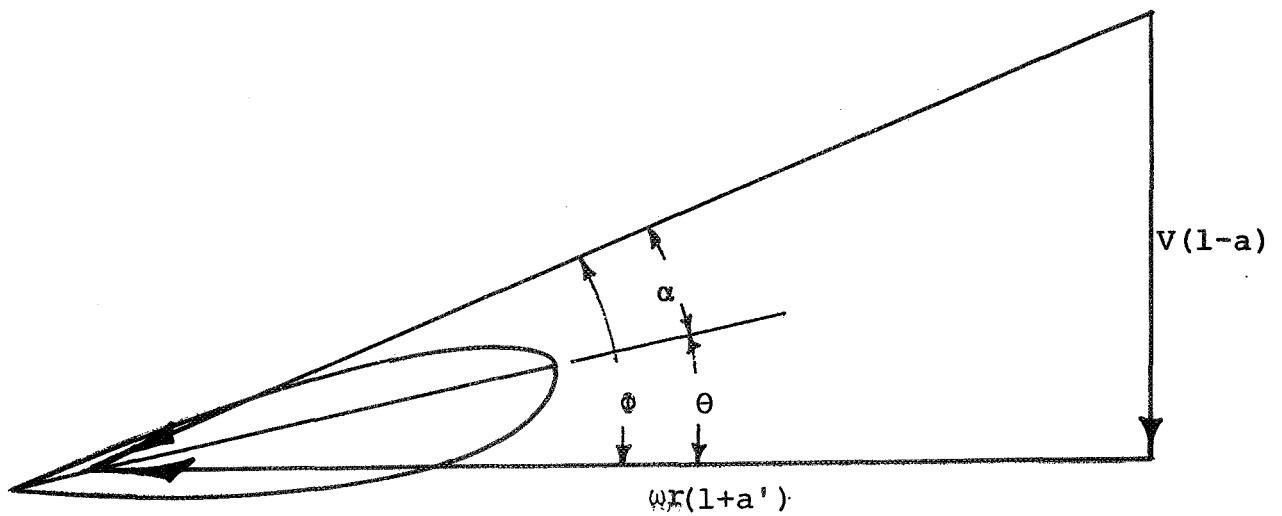


(c) Suction

Figure 2 - Concluded.



(a) Streamtube attenuation of axial velocity.



(b) Blade angles

Figure 3 - Blade Element Velocities

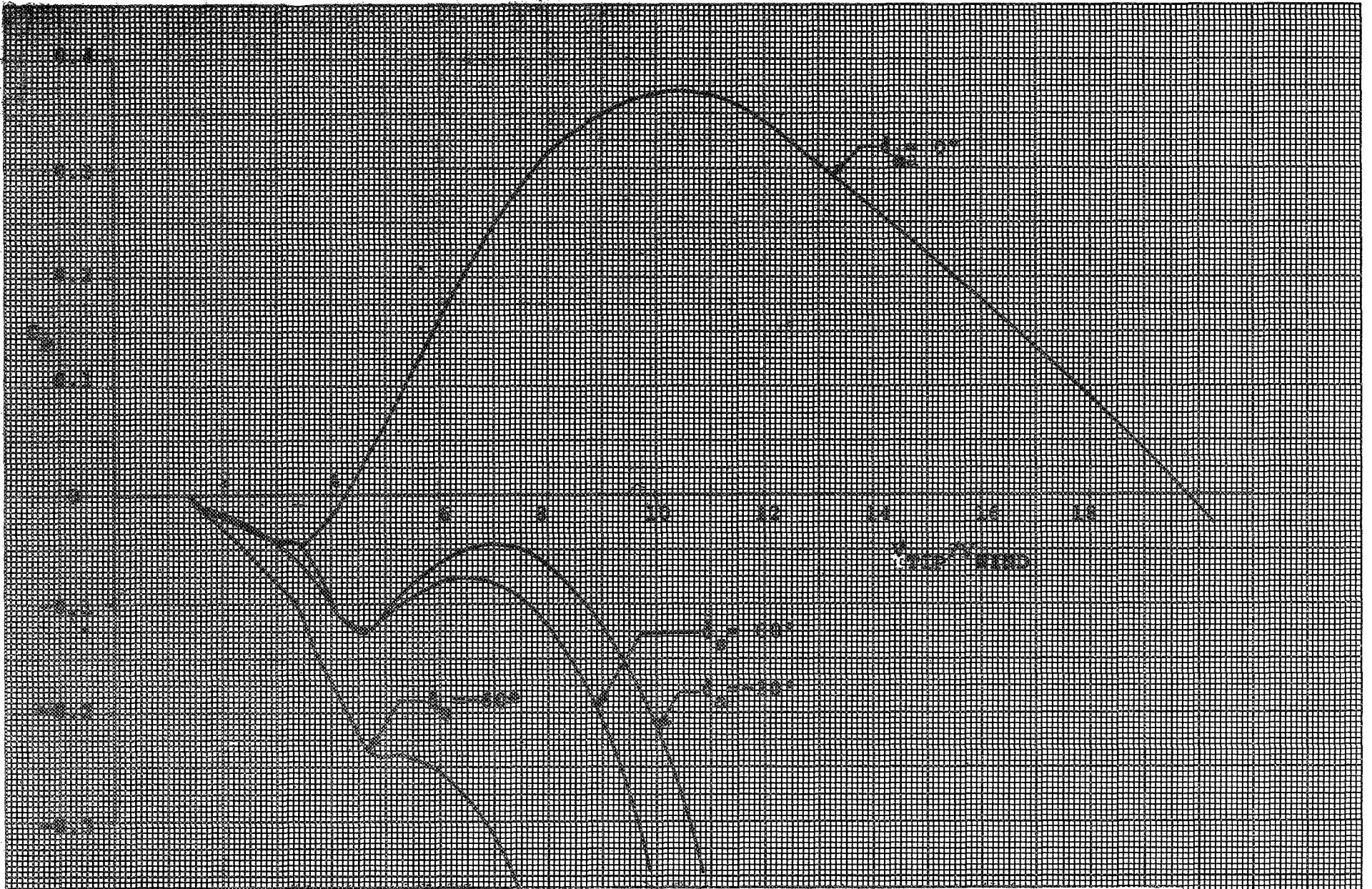


Figure 4 - Effects of Aileron and Spoiler on Power Coefficient.

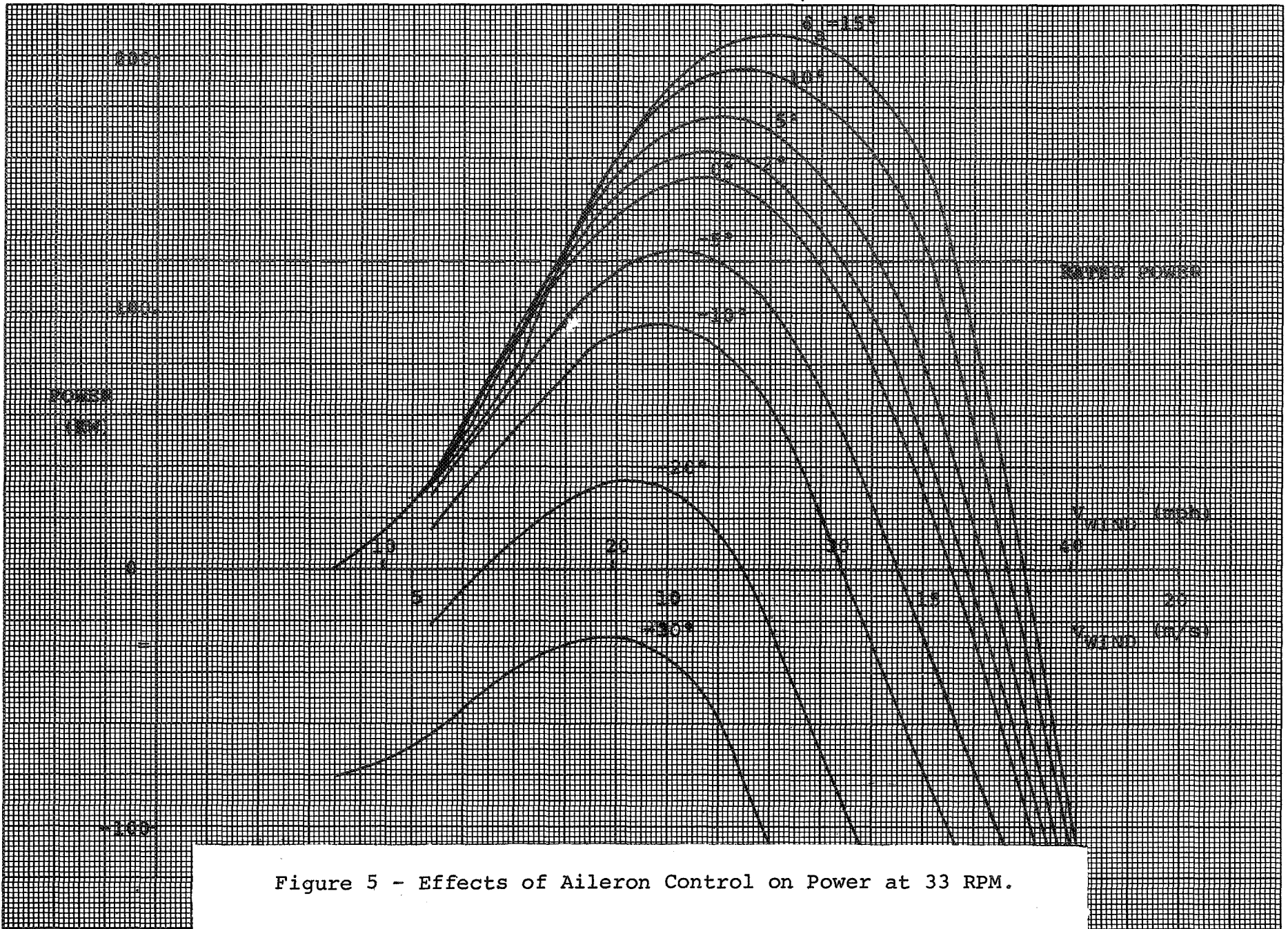
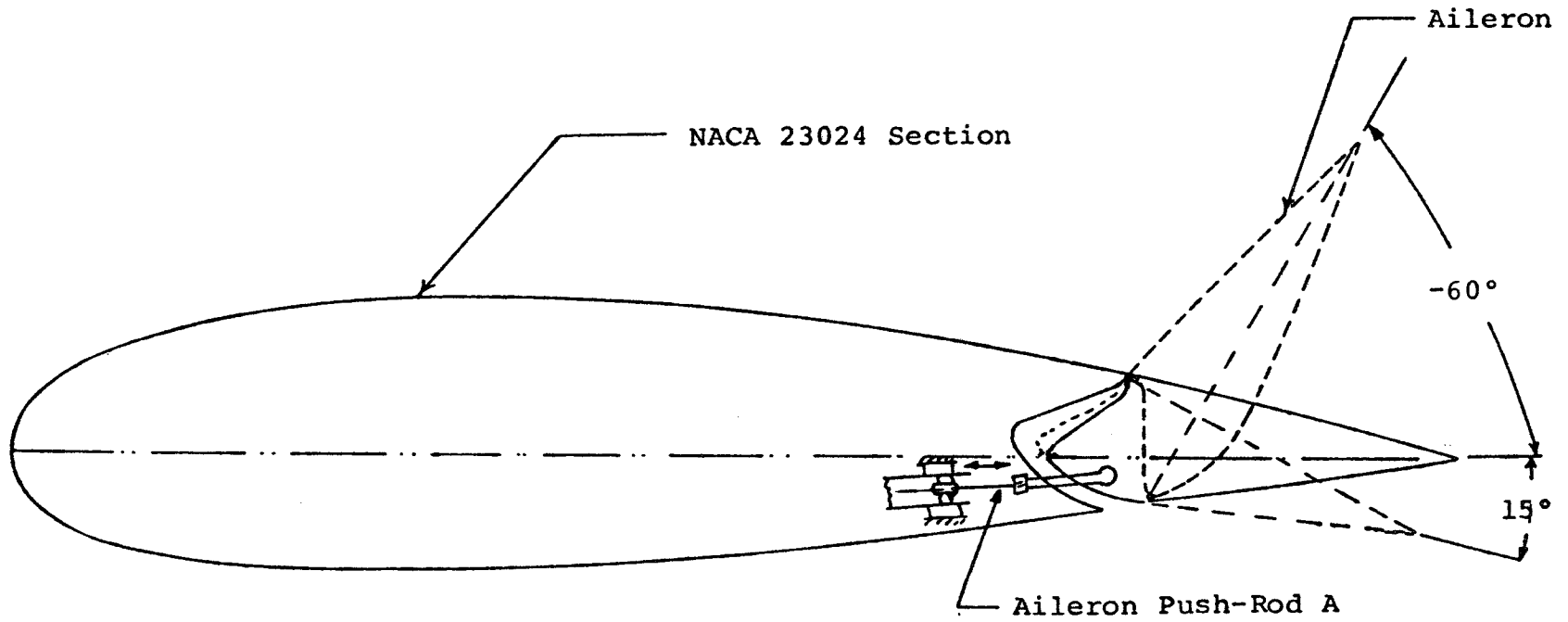
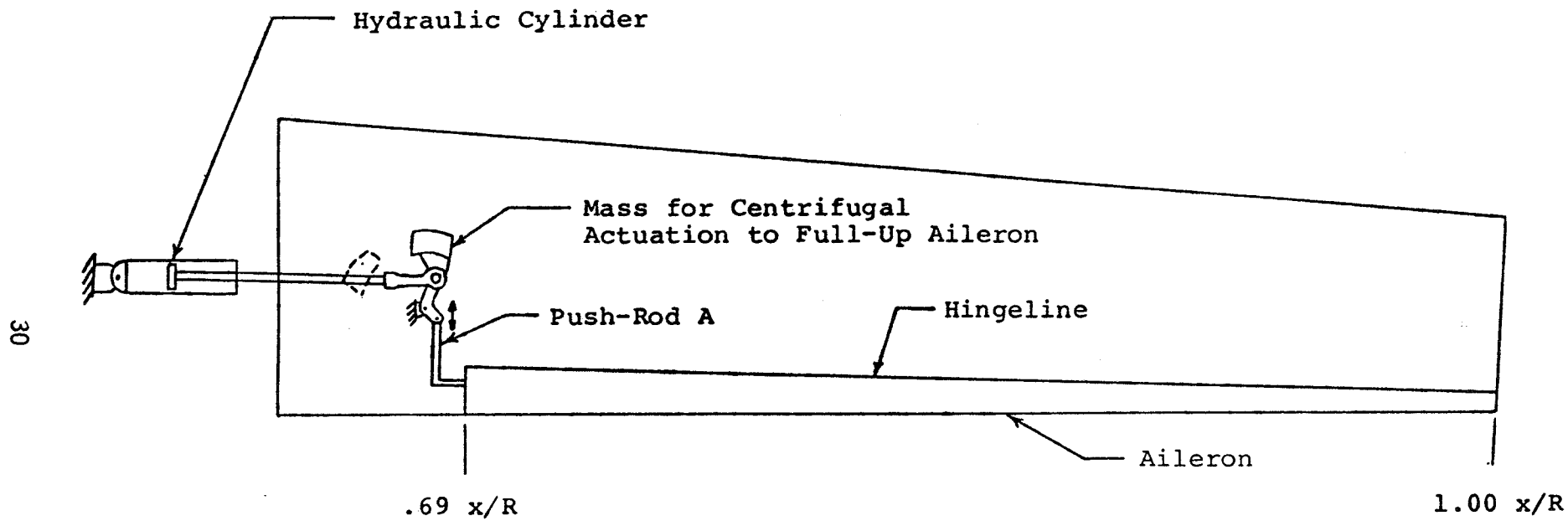


Figure 5 - Effects of Aileron Control on Power at 33 RPM.



(a) Cross-Section at Aileron Root

Figure 6 - Aileron Hardware



(b) Planform Schematic

Figure 6 - Concluded

APPENDIX A

MODIFIED COMPUTER CODE: PROP

Basic Program, "PROP"

The computer program used in the studies conducted under this NASA grant is PROP. This program was originally written by Stel Walker and Robert Wilson at Oregon State University for NASA (ref. 2). Prior to being supplied to Wichita State University, some modifications were made to the program at Lewis Research Center to facilitate its use on the NASA computing system.

After the program was received at WSU, it was modified to permit operation on the university IBM system 370 computer. The program consists of a main program and six subroutines:

Main Program: PROP
Subroutines: SEARCH
CALCZ
TIPLOS
NACAXX
INCREM
BESSEL

As explained in the Performance Analysis section of this report, forces are determined at local stations and then summed for the complete blade. It was determined that it was desirable to use 2% radial increments. The computer program starts at the outboard end of the blades and calculates components of forces for each incremental radial blade element, working inboard to the hub.

Local chord and amount of twist are determined by the subroutine SEARCH using linear interpolation. Subroutine CALC is then called to calculate the axial and rotational interference factors (a and a'), the local angle of attack and lift and drag coefficients. The relationships between angle of attack and lift and drag coefficients are obtained from subroutine NACAXX and modified by subroutines TIPLOS (tip and hub losses) and INCREM (increments of c_l and c_d due to aileron or spoiler deployment).

Convergence Problems and Related Modifications

As can be seen in figure 3, angle of attack is a function of a , and a is a function of the section lift. Thus evaluation of a is an iterative process involving the following steps:

1. Assume initial values of $a = 0$, $a' = 0$.

2. Calculate $\phi = \tan^{-1} \left(\frac{1-a}{1+a'} \right) \frac{V}{r\omega}$ (A1)

3. Calculate $\alpha = \phi - \theta$ (A2)

4. Calculate c_l and c_d as functions of α , including any increments due to spoiler or aileron deflection.

5. Calculate $c_y = c_l \cos \phi + c_d \sin \phi$ (A3)

and $c_x = c_l \sin \phi - c_d \cos \phi$ (A4)

6. Calculate $a = \frac{\frac{Bc}{\pi r} c_y}{8 \sin^2 \phi + \frac{Bc}{\pi r} c_y}$ (A5)

7. Calculate $a' = \frac{\frac{Bc}{\pi r} c_x}{8 \sin \phi \cos \phi}$ (A6)

8. Compare a or a' to previous values to check for convergence. If not converged, return to step 2 and repeat.

This process had been programmed in subroutine CALC to perform the iteration up to 40 times with damping applied on the fourth, tenth, and fifteenth cycles. It was found that at tip speed ratios, X , of more than 15, the average values of a were predicted to be greater than 0.5 for the straight blade at zero pitch angle. For blades with negative or positive loading outboard-- as with tip pitched, ailerons deflected, or spoilers deployed--high values of a were obtained at lower values of X , with local values of $a=1.0$ (or greater) being obtained. While these unrealistic values were usually obtained at low wind speeds outside the normal operating range of the rotors, it was felt that they cast doubt on all performance predictions.

In order to improve calculation of a , the possible number of iterations was increased to 50, damping was applied to each cycle, and local values of a were limited to $-0.5 \leq a \leq 0.5$. Also, an optional procedure was made available which disregarded the induced velocity by setting $a=0$. Figure A-1 compares the results of calculations with (1) a unlimited, (2) $-0.5 \leq a \leq 0.5$, and (3) $a=0$. For the cases shown here, methods (1) and (2) give the same C_p .

Elements of force in the plane of rotation (producing torque) and normal to the rotor plane (producing thrust) are determined by iteration at both ends and at the center of 2% span blade section. The forces are integrated across the section using Simpson's rule and then simply summed to give total quantities for the blades.

Airfoil Characteristics Subroutine, "NACAXX"

Airfoil aerodynamic characteristics used in the PROP computer code are made available to the computer in the form of subroutine NACAXX. This technique permits the program user to develop the aerodynamic information in a form most suited to his own needs, or most compatible with available data. The task of the subroutine is to determine lift and drag coefficients for a given angle of attack, and to return these coefficients to the main program. In subroutine NACAXX used for the present performance studies of the NASA MOD-0 wind turbine, the aerodynamic characteristics of the NACA 23024 airfoil are stored as a set of algebraic equations, with logic to branch to the equation appropriate for a particular angle of attack range. The angle of attack at a given station is calculated from wind speed, angular speed, radius, and induced factor, a .

In order to analyze an airfoil with a control surface, it is necessary to identify geometric characteristics of the control surface, such as control surface chord and deflection, as well as airfoil angle of attack. In addition, it is desirable to store information concerning control surface hinge moments so that control surface actuation loads may be calculated. In the present research, it was decided that control surface data should be treated as increments to be applied to the basic airfoil characteristics. There were two reasons for adopting this procedure: first, no data were available for the NACA 23024 section with spoilers and ailerons; and second, a control surface incremental subroutine would have application to a variety of airfoils with minimal change.

Incremental Subroutine, "INCREM"

This subroutine receives control surface type, control surface chord, and deflection angle as input information. Output information is incremental lift coefficient, incremental drag coefficient, and control surface hinge moment coefficient. The incremental data are added to the basic airfoil coefficients, so that net or total coefficients are returned to the main program for evaluating blade element performance.

The incremental data used in this subroutine were obtained from wind tunnel experiments conducted on a 21% thick airfoil at WSU, specifically the LS(1)-0421 airfoil as documented in reference 3. Figures A-2 and A-3 show incremental data from the reference for lift and drag coefficients, and control surface hinge moment data as a function of control surface deflection and angle of attack. These incremental effects should be reasonable for the NACA 23024 and other airfoils of similar thickness. For sections less than 15% thick, more appropriate data should be used.

The forms selected for the equations used to fit the incremental control surface data have been designed to have rather broad applicability, in terms of control surface chord, even though the present data are obtained from experiments with 20% chord ailerons and 10% chord spoiler, respectively. The resulting equations are believed to be applicable to control surfaces with chord lengths differing by as much as 50% from the source data values, but could lead to serious errors for larger chord differences.

Furthermore, the spoiler data are from experiments with a spoiler hinge-line location of 70% chord. While using the present data base to approximate spoiler characteristics for hingelines from 60% to 90% chord would probably not result in large errors, hingeline locations forward of 50% would be expected to produce large errors, since it is known that spoilers are much more effective at forward locations.

Within these constraints, the forms chosen for the incremental equations will have reasonable applicability. The coefficients should be adjusted based on more appropriate experimental data, when such data are available.

Aileron Increments

Lift:

$$\left. \begin{aligned} \Delta c_l &= \frac{c_a}{c} (11.5 \sin \delta_a - 5 \sin^2 \delta_a) \\ 0^\circ \leq \delta_a \leq 60^\circ, \quad |\alpha| \leq \alpha_{stall}^* \end{aligned} \right\} \quad (A7)$$

$$\left. \begin{aligned} \Delta c_l &= \frac{c_a}{c} (11.5 \sin \delta_a + 3.35 \sin^2 \delta_a) \\ -60^\circ \leq \delta_a \leq 0^\circ, \quad |\alpha| \leq \alpha_{stall} \end{aligned} \right\} \quad (A8)$$

Drag:

$$\left. \begin{aligned} \Delta c_d &= \frac{c_a}{c} (1.05 \sin^2 \delta_a) \\ 0^\circ \leq \delta_a \leq 60^\circ, \quad |\alpha| \leq \alpha_{stall} \end{aligned} \right\} \quad (A9)$$

$$\left. \begin{aligned} \Delta c_d &= \frac{c_a}{c} (0.65 \sin^2 \delta_a) \\ -60^\circ \leq \delta_a \leq 0^\circ, \quad |\alpha| \leq \alpha_{stall} \end{aligned} \right\} \quad (A10)$$

$$(\alpha_{stall}^* = 17^\circ)$$

Hinge Moment:

$$c_h = \frac{c_a}{c} (-.0035 - .0542\alpha - 2.00 \sin \delta_a) \left. \vphantom{c_h} \right\} \quad (A11)$$
$$0^\circ \leq \delta_a \leq 60^\circ, \quad |\alpha| \leq \alpha_{\text{stall}}$$

$$c_h = \frac{c_a}{c} (-.0035 - .0542\alpha - 2.95 \sin \delta_a) \left. \vphantom{c_h} \right\} \quad (A12)$$
$$-60^\circ \leq \delta_a \leq 0^\circ, \quad |\alpha| \leq \alpha_{\text{stall}}$$

To determine overall hinge moment required to actuate a control surface, integration of local section hinge moments across the span of the control is accomplished in program subroutine CALC, in parallel with other spanwise integrations of blade torque and thrust loads.

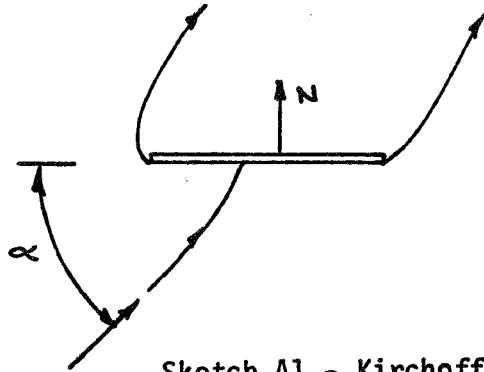
Post-Stall Behavior of Airfoil with Control Surface

Post-stall characteristics of airfoils have been investigated for only a few section shapes. This lack of data is unfortunate, since fixed pitch wind turbines operate over an angle of attack range from approximately 0° to 90° . The aerodynamic characteristics of the NACA 23024 airfoil as modeled in subroutine NACAXX for angles of attack beyond stall were based upon wind tunnel tests of the symmetric 12% thick NACA 0012 section. For post-stall angles of attack with spoiler, it is assumed that the spoiler effectiveness vanishes and that the basic section data apply. This assumption is believed to be reasonable since for high angles of attack, the airfoil will separate in front of the spoiler, rendering it nearly ineffective.

For an airfoil with aileron deflected, on the other hand, the lower surface shape is changed and the lift and drag will be different, even for 90° angle of attack. Since no experimental data for airfoils with ailerons at extreme angles of attack are available, a model was developed for the present study based upon theoretical results from potential flow analysis of flat plates using free streamline techniques. Theoretical results for Kirchoff flow, modified by correcting to a more realistic base pressure are used to develop aileron loads for post-stall cases (see ref. A2; see Sketch A2, p. 37).

The normal force for this flow is given by:

$$N = c_n \frac{1}{2} \rho V^2 c \quad (A13)$$



Sketch A1 - Kirchoff Flow

where

$$c_n = \frac{2\pi \sin(\alpha)}{4 + \pi |\sin(\alpha)|} \quad (A14)$$

For $\alpha = 90^\circ$, equation (A14) gives $c_n = 0.88$. From two-dimensional experiments $c_n \approx 2$. The discrepancy between theory is primarily because the base pressure is not modeled properly by the Kirchoff theory. To correct for this effect, a correction factor K is introduced.

$$c_n = K \frac{2\pi \sin(\alpha)}{4 + \pi |\sin(\alpha)|} \quad (A15)$$

where

$$K = \frac{2.0}{.88} = 2.27$$

This equation (A15) will be used to calculate the normal force for a deflected aileron at angles of attack beyond stall, where no experimental data are available. The load distribution will be assumed uniform over the aileron. The loading on the portion of the airfoil forward of the aileron will be calculated in the usual way, using data from SUBROUTINE NACAXX. The steps in the total calculation process are:

1. Obtain c_l and c_d as a function of α for the airfoil without aileron from NACAXX.
2. Transform lift and drag coefficients to chordwise and normal force coefficients:

$$c_c = c_d * \cos(\alpha) - c_l * \sin(\alpha) \quad (A16)$$

$$c_n = c_l * \cos(\alpha) + c_d * \sin(\alpha) \quad (A17)$$

3. Calculate the contributions of the area forward of the aileron:

$$c_{c1} = c_c * (1 - c_a/c) \quad (A18)$$

$$c_{n1} = c_n * (1 - c_a/c) \quad (A19)$$

4. Calculate the aileron normal force coefficient, and resolve into components parallel and perpendicular to the airfoil chord:

$$c_{n2} = \frac{2.27 * 2\pi * \sin(\alpha + \delta_a)}{4 + \pi * |\sin(\alpha + \delta_a)|} \quad (A20)$$

normal component:

$$\Delta c_{na} = c_{n2} * \frac{c_a}{c} * \cos(\delta_a) \quad (A21)$$

chordwise component:

$$\Delta c_{ca} = c_{n2} * \frac{c_a}{c} * \sin(\delta_a) \quad (A22)$$

5. Calculate aileron hinge moment:

$$c_h = -\frac{c_{n2}}{2} \quad (A23)$$

(Assumes uniform load distribution on aileron.)

6. Calculate airfoil plus aileron force coefficients:

$$c_n = c_{n1} + \Delta c_{n_a} \quad (A24)$$

$$c_c = c_{c1} + \Delta c_{c_a} \quad (A25)$$

7. Convert to lift and drag coefficients:

$$c_l = c_n * \cos(\alpha) - c_c * \sin(\alpha) \quad (A26)$$

$$c_d = c_c * \cos(\alpha) + c_n * \sin(\alpha) \quad (A27)$$

(These are the net section lift and drag coefficients, including aileron effects.)

8. Return to main program.

Spoiler Increments

Lift:

$$\left. \begin{aligned} \Delta c_l &= \frac{c_s}{c} (-9.9 \sin \delta_s) \\ 0^\circ \leq \delta_s \leq 60^\circ, \quad |\alpha| \leq \alpha_{stall} \end{aligned} \right\} \quad (A28)$$

$$\Delta c_l = 0, \quad |\alpha| > \alpha_{stall} \quad (A29)$$

Drag:

$$\left. \begin{aligned} \Delta c_d &= \frac{c_s}{c} (0.93 \sin^2 \delta_s) \\ 0^\circ \leq \delta_s \leq 60^\circ, \quad |\alpha| \leq \alpha_{stall} \end{aligned} \right\} \quad (A30)$$

$$\Delta c_d = 0, \quad |\alpha| > \alpha_{stall} \quad (A31)$$

Hinge Moment:

$$c_h = \frac{c_s}{c} (0.175\alpha - 6.7)(\sin^2 \delta_s) \quad \left. \vphantom{c_h} \right\} \quad (A32)$$
$$0^\circ \leq \alpha \leq \alpha_{\text{stall}}$$

$$c_h = \frac{c_s}{c} (0.075\alpha - 6.7)(\sin^2 \delta_s) \quad \left. \vphantom{c_h} \right\} \quad (A33)$$
$$-\alpha_{\text{stall}} \leq \alpha < 0^\circ$$

$$c_h = 0, \quad |\alpha| > \alpha_{\text{stall}} \quad (A34)$$

Expanded Output Modifications

In order to facilitate analysis of effects of spoiler or aileron deflections on wind turbine performance, the output of the computer program was expanded.

The computer program output was modified to provide two alternative types of display of the performance results. The "long print-out" shows local values of velocity, angle of pitch, angle of attack, coefficients of lift and drag, and the resulting local contributions to torque, thrust, and a . Integrated results are also printed including torque, thrust, power, c_p , average a , and hinge moment. The "short print-out" displays only the integrated values.

The reason for the long print-out is that it permits an investigator to examine local wind angles and angles of attack across the radius from hub to tip, the resulting blade loading and induced effects.

An additional optional print-out was added to the program during the present research. At each radial station, the computer seeks to satisfy continuity and momentum relationships by an iterative procedure involving a , the induced velocity factor, net angle of attack on the blade section, and the resulting section lift and drag coefficients. In order to examine this iterative process, an optional command causes the printer to list each successive estimate of local α , c_l , c_d , and the factor a . If a does not converge in the 50 iterations a warning is printed on the output sheet.

Hinge Moment

Hinge moments for the spoiler studies were obtained directly from the wind tunnel data of reference A3. For the aileron studies, however, hinge moment data from this reference are not directly applicable, because of the large difference in airfoil camber between the two sections, especially near the trailing edge. The equation for hinge moment coefficient is given by:

$$c_h = c_{h0} + c_{h\alpha} \alpha + c_{h\delta} \delta \quad (\text{A35})$$

where:

c_h = hinge moment coefficient

c_{h0} = hinge moment coefficient at $\alpha = 0^\circ$ and $\delta = 0^\circ$
(a function of camber)

$c_{h\alpha}$ = rate of change of hinge moment with alpha, obtained from
the data of reference 5

$c_{h\delta}$ = rate of change of hinge moment with aileron deflection,
from reference 5

Since the value of c_{h0} depends on camber of the section, and no experimental data were available for the NACA 23024 section, a value for this parameter was obtained by integration of the pressure distribution over the airfoil trailing edge region using theoretical data from reference A4.

Computer Program Listing

A listing of the computer program with all the modifications described above follows:


```

WRITE (KP,63)
GO TO (84,85,86),MCON
84 WRITE (KP,64) TIPICH, TIPL
GO TO 89
85 WRITE (KP,65) SPAN, PCTSPN, DEFL
WRITE (KP,67)
GO TO 89
86 WRITE (KP,66) SPAN, PCTSPN, DEFL
WRITE (KP,68)
89 GO TO (19,21,22),KFLAG
19 WRITE (KP,78)
GO TO 91
21 WRITE (KP,79)
GO TO 91
22 WRITE (KP,83)
91 IF (IPRINT.EQ.1) GO TO 90
WRITE (KP,77)
WRITE (KP,70)
WRITE (KP,74)
WRITE (KP,75)
WRITE (KP,76)
WRITE (KP,70)
90 DO 500 NO=1,NINC
IF (IPRINT.EQ.2) GO TO 13
WRITE (KP,69)
WRITE (KP,71)
WRITE (KP,72)
WRITE (KP,73)
WRITE (KP,69)
13 IF (MODE.EQ.1) GO TO 6
IF (MODE-2) 499,7,499
6 VDEL=INCVEL
V=V+VDEL
GO TO 8
7 RPMINC=INCRPM
OMEGA=OMEGA+RPMINC
8 PI=3.141593
RADEG = PI/180.
FPSMPH = 88./60.
ISTOP=0
SCALE=1.
CONTINUE
R = R*SCALE
HB = HB*SCALE
OMEGA = OMEGA/SCALE
DO 4 I=1,NF
CIM (I)=0.3048*SCALE*CI (I)
4 CI (I) = CI (I)*SCALE
IREAD=0
C STORE INITIAL VALUES
2 S1 = R
S2 = DR
S3 = HB
S4 = THETP

```



```

S5 = V
S6 = OMEGA
S7 = SI
C SI IS CONOING ANGLE (PSI)
COSSI=COS(SI*RADEG)
CS2=COSSI*COSSI
W=R*COSSI*OMEGA*PI/30.
X=W/V/FPSMPH
C
C ..... INITIALIZATION AND CONSTANT PARAMETER CALCULATIONS .....
C
THETP=-THETP*RADEG
V=V*FPSMPH
OMEGA=OMEGA*PI/30.
SI=SI*RADEG
SUM1 = 0.0
SUM2 = 0.0
QX=0.0
QY=0.0
TX=0.0
TY=0.0
PX=0.0
PY=0.0
AK=1.
ASTOP=0.0
C INDUCED VELOCITY FACTORS ARE SET EQUAL TO ZERO TO BEGIN ITERATION
A=0.0
AP=0.0
HMOM=0.0
CONTRL=3.0
C 'CONTROL' COUNTS STEP IN 3-STEP SIMPSON RULE INTEGRATION
RHO=0.0023769199*EXP(-0.297*H/10000.)
RX=R
C CORRECT FOR CONING
R=R*COSSI
REF =BO*R
DR=DR*R
DRO=DR
HB=HB*COSSI
C 'NN' IS NUMBER OF STEPS ACROSS SPAN, DETERMINED FROM INPUT VALUE
C OF DR
NN=(R-HB)/DR+3.
IF(IREAD.GT.0) GO TO 5
DO 11 I=1,NF
RR(I)=R*RR(I)/100.
11 THETI(I)=THETI(I)*RADEG
5 CONTINUE
C SET R LOCAL EQUAL TO RMAX
RL=R
C
C ..... NUMERICAL INTEGRATION FROM TIP TO HUB .....
C
CAT=1.
IF(GO.EQ.2.) CAT=2.

```

```

CLFA=1.
IF(GO.LT.2.) GO TO 563
IF(GO.EQ.3.) CLFA=0.0
IF (IREAD.GT.0) GO TO 211
CALL SEARCH (RL,CX1,THETX1,CA,CS,DA,DS)
211 C=CX1
    THET = THETX1
    CALL CALC(RL,C,THET,QX,TX,A,AP,F,CLFA,CAT,CL,CD,ALFA,CH,CA,CS,DA,
2DS)
C RE-INITIALIZE 'A'
563 A=0.0
    CAT=0.0
C BEGIN MARCHING ACROSS SPAN FROM TIP TO HUB
DO 100 L=1,NN
C DO NOT MARCH INSIDE HUB
IF((RL-HB).GE.DR) GO TO 50
ASTOP=ASTOP+1.
IF(ASTOP.GE.2.) GO TO 93
DR=(RL-HB)
50 IF(GO.LT.3.) GO TO 311
C TEST FOR STEP IN 3-POINT SIMPSON
IF(CONTRL.EQ.0.0) GO TO 311
TIP=RL-DR
IF(TIP.GT.REF) GO TO 312
IF(CONTRL.EQ.2.) GO TO 311
DR=(RL-REF)
CLFO=(REF-TIP)/(RL-TIP)
CLF=.5*CLFO
CONTRL=1.
GO TO 311
312 CLF=0.0
311 DR2=DR/2.
    DT6=DR/(6.*COSSI)
C INCREMENT 'R' BY 'DR/2'
    RL=RL-DR2
    IF(CONTRL.EQ.0.0) CLF=1.
    IF(CONTRL.EQ.2.0) CLF=(CLFO+1.)/2.
    IF (IREAD.GT.0) GO TO 202
C FIND LOCAL CHORDS AND ANGLES
CALL SEARCH (RL,CHD(1,L),THETX(1,L),CA,CS,DA,DS)
202 C=CHD(1,L)
    THET = THETX(1,L)
C CALCULATE VALUES AT R+DR/2 STATION
CALL CALC(RL,C,THET,QXP1,TXP1,A,AP,F,CLF,CAT,CL,CD,ALFA,CH,CA,CS,
2DA,DS)
C INCREMENT R BY DR/2 AGAIN(TOTAL INCREMENT = DR)
    RL=RL-DR2
    IF(CONTRL.EQ.0.0) CLF=1.
    IF(CONTRL.EQ.1.0) CLF=CLFO
    IF(CONTRL.EQ.2.0) CLF=1.0
    IF (IREAD.GT.0) GO TO 203
C FIND LOCAL CHORDS AND ANGLES
CALL SEARCH (RL,CHD(2,L),THETX(2,L),CA,CS,DA,DS)
203 C=CHD(2,L)

```

```

      THET = THETX(2,L)
C      CALCULATE VALUES AT R+DR STATION
      CALL CALC(RL,C,THET,QXP,TXP,A,AP,F,CLF,CAT,CL,CD,ALFA,CH,CA,CS,DA,
2DS)
C      THETA=LOCAL BLADE TWIST+PITCH SETTING
      THETA=THET+THETP
      PCRL=(100.)*RL/R
      RLM=0.3048*RL
      CM=0.3048*C
C      NEXT 4 STEPS INTEGRATE TORQUE,THRUST AND POWER,USING 3-POINT
C      SIMPSONS RULE
C      3 VALUES ARE AT R,R+DR/2,AND R+DR
      QYX=DT6*(QX+4.*QXP1+QXP)
      QY=QY + QYX
      TY=TY+DT6*(TX+4.*TXP1+TXP)
      PY=PY+OMEGA*QYX
      HMOM=HMOM+HMF*DR/COSSI
      IF(CONTRL.EQ.2.) CONTRL=0.0
      IF(CONTRL.EQ.0.0) GO TO 313
      IF((RL-TIP).EQ.0.0) GO TO 313
      IF(CONTRL.EQ.1.) DR=REF-TIP
      IF(CONTRL.EQ.1.) CONTRL=2.
      GO TO 314
313  DR=DRO
314  CONTINUE
      QX=QXP
      TX=TXP
C      NEXT 3 STEPS CALCULATE TERMS TO EVALUATE AVERAGE A ('AVA')
C      OVER THE SPAN
C      'AVA' STEP BELOW COMPLETES THE CALCULATION
      AREA = DR*(2.*RL+DR)
      SUM1 = SUM1+AREA
      SUM2 = SUM2+(1.-A)*AREA
      IF(IPRINT.EQ.2) GO TO 100
29  GO TO (33,31,31),MCON
33  CH=0.
31  WMS=W*0.447040
      WRITE(KP,80) PCRL,RLM,CM,THETA,ALFA,WMS,CL,CD,CH,QXP,A,AP
100  CONTINUE
93  CONTINUE
      CTY=TY/(.5*RHO*V**2*PI*RX**2)
      CPY=PY/(.5*RHO*V**3*PI*RX**2)
      TP=PY/737.6
      PWR=TP*PFACT(KW)
      AVA=1.-SUM2/SUM1
C  RESTORE INITIAL VALUES FOR POSSIBLE RERUN
      IF(IREAD.EQ.1) GO TO 105
      DO 104 I=1,NF
      RR(I)=100.*RR(I)/R
104  THETI(I)=THETI(I)/RADEG
      IREAD=1
105  CONTINUE
      R = S1
      DR = S2

```

```

HB = S3
THETP = S4
V = S5
OMEGA = S6
SI = S7
S8 = X
VMS=0.447040*V
QYNM=QY*1.355833
TYN=4.44827*TY
CQ=CPY/X
HMOM=HMOM*.7376
IF(IPRINT.EQ.2) GO TO 490
WRITE(KP,77)
WRITE(KP,70)
WRITE(KP,74)
WRITE(KP,75)
WRITE(KP,76)
WRITE(KP,70)
490 WRITE(KP,81) V, VMS, OMEGA, X, THETP, QYNM, TP, CPY, TYN, CQ, HMOM, AVA
IF(IPRINT.EQ.2) GO TO 500
WRITE(KP,813)
500 CONTINUE
GO TO 502
499 WRITE(KP,815)
GO TO 502

```

```

C
C ..... FORMATS FOR INPUT AND OUTPUT STATEMENTS .....

```

```

C
10 FORMAT(4F10.3)
20 FORMAT(7F10.5)
30 FORMAT(2F10.3,I2,8X,F10.2,I4)
40 FORMAT(5F10.3)
41 FORMAT(5A2,I5,6F10.5)
42 FORMAT(6I10)
60 FORMAT('1',40X,'PERFORMANCE OF A WIND-AXIS WIND TURBINE')
61 FORMAT(' ',42X,'CALCULATED BY MODIFIED PROP PROGRAM')
62 FORMAT('0',8X,'BLADE SECTION - ',5A2,5X,'NO. BLADES = ',F2.0,7X,'R
2 RADIUS = ',F5.2,' METERS CONING ANGLE = ',F4.1,' DEGREES')
63 FORMAT('0',8X,'METHOD OF CONTROL --')
64 FORMAT(' ',30X,'TIP SECTION PITCH, ANGLE OF PITCH = ',F5.1,' DEGREE
4S TIP SECTION LENGTH = ',F4.1,' METERS')
65 FORMAT(' ',30X,'AILERONS, SPAN = ',F5.1,' METERS (OUTBOARD',F5.1,
5' PERCENT) DEFLECTION = ',F6.1,' DEGREES')
66 FORMAT(' ',30X,'SPOILERS, SPAN = ',F5.1,' METERS (OUTBOARD',F5.1,
6' PERCENT) DEFLECTION = ',F6.1,' DEGREES')
67 FORMAT('0',35X,'AILERON CHORD IS 20% OF LOCAL BLADE CHORD')
68 FORMAT('0',30X,'SPOILER CHORD IS 10% OF LOCAL CHORD - - HINGED AT
*70% CHORD')
69 FORMAT(' ',3X,3(' |-----'), '|-----|-----',5(' |-----'),
92(' |-----'), '|')
70 FORMAT(' ',3X,3(' |-----'), '|-----|-----',3(' |-----'),
7' |-----|-----|-----|')
71 FORMAT(' ',3X,'| BLADE | RADIUS | LOCAL | PITCH | ANGLE OF | RES
1 ULTANT| COEF. | COEF. | HINGE | TORQUE | A | A'' |')

```

```

72 FORMAT(' ',3X,'| STATION |          | CHORD | ANGLE | ATTACK |VEL
2OCITY | OF | OF | MOMENT | INCREMENT| | |')
73 FORMAT(' ',3X,'| (PERCENT)| (METERS) | (METERS) | (DEG.) | (DEG.) | (M
3/SEC) | LIFT | DRAG | COEF. | (N-M) | | |')
74 FORMAT(' ',3X,'| FREESTREAM |ANGULAR |TIP-SPEED| PITCH | TORQ
4UE | POWER | POWER | THRUST | TORQUE |HINGE MOM| A |')
75 FORMAT(' ',3X,'| WIND SPEED | SPEED | RATIO | ANGLE |',9X,
5'|',9X,'| COEF. |',10X,'| COEF. |PER BLADE| (AVE) |')
76 FORMAT(' ',3X,'| (MPH) | (M/S) | (RPM) | X | (DEG) | (N-
6M) | (KW) | CP | (NEWTON) | CQ | (N-M) | |')
77 FORMAT('0',//,6X,'INTEGRATED RESULTS --',//)
78 FORMAT('0',40X,'NOTE:"A" IS ZERO ; INDUCED VELOCITIES ARE IGNORED'
*//)
79 FORMAT('0',40X,'NOTE: -0.5.LE. A .LE.+0.5'//)
80 FORMAT(' ',F10.1,F10.2,F11.3,F8.1,F9.1,F10.1,F9.2,F11.3,F10.3,F10.
81,F9.3,F9.4)
81 FORMAT('0',F9.1,F11.2,F8.1,F10.3,F8.1,F12.1,F9.2,F10.3,F12.1,F8.3,
1F10.3,F8.3)
83 FORMAT('0',40X,'NOTE:"A" IS NOT LIMITED'//)
813 FORMAT('1')
815 FORMAT('0',2X,'MODE IN ERROR, PROGRAM STOPPED')
502 CONTINUF

```

```

C
STOP
END
CCCCCCCCCCCCCCCCCCCCCCCCCCCCCCCCCCCCCCCCCCCCCCCCCCCCCCCCCCCC
SUBROUTINE SEARCH (RL,C,THET,CA,CS,DA,DS)

```

```

C
C ..... SEARCH - DETERMINES THE CHORD AND THE TWIST ANGLE AT
C A GIVEN RADIUS ALONG THE SPAN. IT UTILIZES A LINEAR
C INTERPOLATION TECHNIQUE.
C

```

```

COMMON /HOPE/ R,DR,HB,B,V,X,THETP,AMOD,H,SI,GO,OMEGA,RHO,VIS,HL,
1 PI,RX,W,NPROF,APF,RADEG,COSSI,CS2,NF,RR(50),CI(50),THETI(50),
2T1,T2,T3,T4,T5,T6,T7,T8,XETA,HH,BO,CAI(50),CSI(50),DAI(50),DSI(50)
3,MCON,HMF,KFLAG
RRV=RL
IF(RRV.EQ.RR(1)) GO TO 50
C LOCATE FIRST R IN ARRAY LESSTHAN RLOCAL, AND BRANCH TO
C INTERPOLATION STEPS
DO 20 I=2,NF
IF(RRV.GE.RR(I)) GO TO 10
C IF RLOCAL IS LESS THAN LAST VALUE IN TABLE, SET R=LAST VALUE
IF(I.EQ.NF) GO TO 30
20 CONTINUE
10 J=I+1
C COMPUTE INTERPOLATED VALUE
PER=(RRV-RR(J-1))/(RR(J-2)-RR(J-1))
C=PER*(CI(J-2)-CI(J-1))+CI(J-1)
THET=PER*(THETI(J-2)-THETI(J-1))+THETI(J-1)
CA=PER*(CAI(J-2)-CAI(J-1))+CAI(J-1)
CS=PER*(CSI(J-2)-CSI(J-1))+CSI(J-1)
DA=PER*(DAI(J-2)-DAI(J-1))+DAI(J-1)
DS=PER*(DSI(J-2)-DSI(J-1))+DSI(J-1)

```



```

C      THETA IS LOCAL BLADE PITCH ANGLE
      ALPHA=PHI-THETA
C
C      ..... CALCULATION OF SECTIONAL LIFT AND DRAG COEFFICIENTS
C
C      CALCULATE RESULTANT VELOCITY ('W')
550    W=V*SQRT(((1.-A)*COSSI)**2+((1.+AP)*XL)**2)
      CALL NACAXX(RL,RX,SI,ALPHA,CL,CD,W)
      GO TO(22,21,21),MCON
C      CALCULATE CONTROL SURFACE INCREMENTAL CL, INCREMENTAL CD, AND CH
21    CALL INCREM(ALPHA,CL,CD,CH,CA,DA,CS,DS,C)
22    ALFA=ALPHA*57.29578
      IF(MCON.EQ.1) CH=0.
800   CONTINUE
      IF(GO.LT.3.) GO TO 666
      CL=CLF*CL
      F=1.
      GO TO 667
C
C      ..... CALCULATION OF TIP AND HUB LOSSES .....
C
666   IF(CAT.EQ.1.) F=0.0
      IF(CAT.EQ.1.) GO TO 667
      XXL=ABS(COSPHI/SINPHI)
      XXLO=XXL*R/RL
      CALL TIPLOS(XXL,XXLO,F,B,GO,HL,PI,R,RL,PHI,RH)
C
667   CX=CL*SINPHI-CD*COSPHI
      CY=CL*COSPHI+CD*SINPHI
C      'A MOD' DETERMINES MADEL FOR 'A'.
      IF(AMOD.EQ.0.) GO TO 575
      VBR=SIG8*CY*CS2/(SINPHI**2)
      VAR=SIG8*CX/F/SINPHI/COSPHI
      CAN=F*F+4.*VBR*F*(1.-F)
      IF(CAN.LT.0.0) CAN=0.0
C      'A' IS INDUCED AXIAL VELOCITY FACTOR, 'A' IS INDUCED RADIAL
C      VELOCITY FACTOR.
      A=(2.*VBR+F-SQRT(CAN))/(2.*(VBR+F*F))
C      IF 'APF' IS 1.0, PROGRAM CONVERGES ON 'A', NOT 'AP'.
C      IF 'APF' IS NOT 1.0, PROGRAM CONVERGES ON 'AP', NOT 'A'.
      IF(APF.EQ.1.) GO TO 580
      AP=VAR/(1.-VAR)
      GO TO 580
575   VBR=SIG8*CY*CS2
      VAR=SIG8*CX
      IF(KFLAG.EQ.1) A=0.0
      IF(KFLAG.EQ.1) GO TO 579
      A=VBR/(F*SINPHI**2+VBR)
579   IF(APF.EQ.1.) GO TO 580
      AP=VAR/(F*SINPHI*COSPHI-VAR)
580   CONTINUE
      IF(KFLAG.EQ.3) GO TO 581
      IF(A.GT.0.5) A=0.5
      IF(A.LT.(-0.5)) A=-0.5

```

```

C      ..... DAMPENING OF AXIAL AND ANGULAR INTERFERENCE FACTOR
C      ITERATIONS.
581  CONTINUE
40    A=(A+BETA)*.5
      AP=(AP+DELTA)*.5
30    CONTINUE
C
C      ..... TEST FOR CONVERGENCE .....
C
      IF(APF.EQ.1.) GO TO 70
      IF(ABS(AP-DELTA).LE..001) GO TO 50
      GO TO 10
70    IF(ABS(A-BETA).LE..001) GO TO 50
C      WHEN SPECIAL DIAGNOSTIC PRINT-OUT IS NEEDED, CARDS ARE INSERTED HE
C
10    CONTINUE
      KP=6
      WRITE(KP,79)
79    FORMAT('0',2X,'VALUE OF SLOWDOWN FACTOR, A , IS NOT CONVERGED'/)
50    W=V*SQRT(((1.-A)*COSSI)**2+((1.+AP)*XL)**2)
      CT1=(0.5*RHO*B*C)*(W*W)
      QF=CT1*RL*CX
      TF=CT1*CY*COSSI
      HMF=CH*CT1*CA**2/C
C
      RETURN
      END
CCCCCCCCCCCCCCCCCCCCCCCCCCCCCCCCCCCCCCCCCCCCCCCCCCCCCCCCCCCCCCCCCCCC
SUBROUTINE TIPLOS(U,UO,F,Q,GO,HL,PI,R,RL,PHI,RH)
C
C      ..... TIPLOS - DETERMINES THE TIP AND HUB LOSSES
C      BASED UPON GOLDSTEIN'S THEORY, OR PRANDTL'S THEORY,
C      OR FOR THE CASE OF NO LOSSES.
C
      SUM2=0.0
      SUM=0.0
      AK=1.
      AMM=1.
      AM=0.0
      IF(Q.GT.2.0) GO TO 966
      IF(GO.EQ.0.0) GO TO 200
      IF(GO.EQ.1.0) GO TO 100
      IF(GO.EQ.2.0) GO TO 444
966   IF(GO.EQ.2.0) GO TO 444
200   CONTINUE
      F=(2./PI)*ARCOS(EXP(-(Q*(R-RL))/(2.*RL*SQRT(SIN(PHI)**2+.0001))))
      GO TO 105
444   F=1.0
      GO TO 105
100   IF((ABS(SIN(PHI))).LT..0001) GO TO 200
C
C      .... GOLDSTEINS METHOD.....
C
      DO 10 M=1,3

```



```

V=(2.*AM+1.)
Z0=U0*V
V2=V*V
Z=U*V
Z2=Z*Z
CALL BESSEL(Z,V,AI)
CALL BESSEL(Z0,V,AI0)
IF(Z.GE.3.5) GO TO 300
A=2.*2.
B=4.*4.
C=6.*6.
D=8.*8.
T1VZ=Z2/(A-V2)+(Z2*Z2)/((A-V2)*(B-V2))+(Z2**3)/((A-V2)*(B-V2)*
1(C-V2))+(Z2**4)/((A-V2)*(B-V2)*(C-V2)*(D-V2))
CT1VZ=(V*PI*AI)/(2.*SIN(.5*V*PI))-T1VZ
GO TO 400
300 T0=(U*U)/(1.+U*U)
T2=4.*U*U*(1.-U*U)/((1.+U*U)**4)
T4=16.*U*U*(1.-14.*U*U+21.*U**4-4.*U**6)/((1.+U*U)**7)
T6=64.*U*U*(1.-75.*U*U+603.*U**4-1065.*U**6+460.*U**8-36.*U**10)
1/((1.+U*U)**10)
CT1VZ=T0+T2/V2+T4/(V2**2)+T6/(V2**3)
400 FVU=(U*U)/(1.+U*U)-CT1VZ
SUM=SUM+FVU/V2
IF(AM.NE.0.0) GO TO 1
E=-0.098/(U0**.668)
1 IF(AM.NE.1.0) GO TO 2
E=0.031/(U0**1.285)
2 IF(AM.GT.1.0) E=0.0
SUM2=SUM2+((U0*U0*AMM)/(1.+U0*U0)-E)*(AI/AI0)
AM=AM+1.
AK=((2.*AM-1.)*AK)/(2.*AM)
10 AMM=AK/(2.*AM+1.)
G=(U*U)/(1.+U*U)-(8./(PI*PI))*SUM
CIRC=G-(2./PI)*SUM2
F=((1.+U*U)/(U*U))*CIRC
C
C HUBLOSS CALCULATIONS
C
105 IF(HL.EQ.1.0) GO TO 500
FI=1.0
GO TO 900
500 FI=(2./PI)*ARCOS(EXP(-(Q*(RL-RH))/(2.*RH*SQRT(SIN(PHI)**2+
1.0001))))
900 F=F*FI
RETURN
END
CCCCCCCCCCCCCCCCCCCCCCCCCCCCCCCCCCCCCCCCCCCCCCCCCCCCCCCCCCCCCCCCCCCC
CCCCCCCCCCCCCCCCCCCCCCCCCCCCCCCCCCCCCCCCCCCCCCCCCCCCCCCCCCCCCCCCCCCC
SUBROUTINE BESSEL(Z,V,AI)
C
C ..... BESSEL CALCULATES BESSEL FUNCTIONS FOR THE GOLDSTEIN
C TIP LOSS MODEL.....
C

```

```

S=0.0
AK=0.0
C=1.
DO 30 K=1,10
B=(.25*Z*Z)**AK
D=V+AK
P=1.
5 TK=D-1.
IF(TK.LE.0.0) GO TO 40
P=D*TK*P
D=D-2.
GO TO 5
40 E=P
S=B/(C*E) + S
AK=AK+1.
C=AK*C
30 CONTINUE
AI=((.5*Z)**V)*S
RETURN
END
SUBROUTINE NACAXX(RL,RX,SI,ALPHA,CL,CD,W)
C THIS SUBROUTINE CALCULATES LIFT AND DRAG COEFFICIENTS FOR THE NACA
C 23024 HALF ROUGH AIRFOIL
C AS A FUNCTION OF THE ANGLE OF ATTACK ALPHA (IN RADIANS).
C
Y = ALPHA*180./3.1415927
AALPHA = ABS(ALPHA)
X = ABS(Y)
C
5 CONTINUE
IF(8. .LT. X .AND. X .LT.13.) CD = X/248.8-.01675
IF(-9. .LE. Y .AND. Y .LE. +8.) CD = -2.09050E-6*Y**3 + 7.19578E-5*Y
***2 + 2.26766E-4*X + 9.99331E-3
C
IF(13. .LE. X .AND. X .LT. 160.) CD = 2. - 1.089*(1.57-AALPHA)**2
C
IF(160. .LE. X .AND. X .LE. 180.) CD = 0.04 + 2.8*(AALPHA-3.142)**2
C
C
4 CONTINUE
IF(10. .LE. X .AND. X .LE. 16.) CL = -1.25E-3*X**3 + 4.55953E-2*X**2
* -5.47084E-1*X + 3.04822
C
IF(-12. .LE. Y .AND. Y .LT. 10.) CL = 2.64619E-10*Y**8 + 2.39782E-8*
*Y**7 + 1.03975E-7*Y**6
1-5.54091E-6*Y**5 - 2.20717E-5*Y**4 + 3.11341E-4*Y**3 + 4.59110E-4*Y**
*2 + 8.26369E-2*Y + 1.00579E-1
C
IF(16. .LT. X .AND. X .LE. 90.) CL = 1.1- 1.78*(AALPHA-.7853)**2
C
IF(90. .LT. X .AND. X .LE. 160.) CL = -1.1+ 1.78*(AALPHA-2.356)**2
C
IF(160. .LT. X .AND. X .LE. 172.5) CL = -.763
C

```

```

IF(172.5 .LT. X .AND. X .LE. 180.)CL = .10173*X - 18.3114
C
IF(Y .LT. -12.)CL = -CL
C
RETURN
END
CCCCCCCCCCCCCCCC SUBROUTINE INCREM CCCCCCCCCCCCCCCCCC
C WRITTEN BY W. H. WENTZ AND CYRUS OSTAWARI, WSU, JULY 1979...
C ADJUSTS AIRFOIL COEFFICIENTS FOR DEFLECTION OF SPOILERS OR AILER
SUBROUTINE INCREM(ALPHA,CL,CD,CH,CA,DA,CS,DS,C)
PI=3.141593
Y=ALPHA*180./PI
C CHO DEPENDS ON AIRFOIL CAMBER NEAR TRAILING EDGE.
C THIS VALUE OF CHO IS FOR NACA 230 MEAN LINE AILERONS ONLY!
CHO=-.0035
CH=0.
DAR=DA*PI/180.
DSR=DS*PI/180.
IF(CA.EQ.0.)GO TO 5
C BEGIN AILERON INCREMENT CALCULATIONS
C CHECK FOR POST STALL CONDITION
IF(17..LT.Y.OR.Y.LT.-17.)GO TO 25
IF(0..LE.DA.AND.DA.LE.60.)GO TO 10
IF(-60..LE.DA.AND.DA.LT.0.)GO TO 15
10 DCL=CA/C*(11.5*SIN(DAR)-5.*SIN(DAR)*SIN(DAR))
DCD=1.05*CA/C*SIN(DAR)*SIN(DAR)
CH=CA/C*(CHO-.0542*Y-2.*SIN(DAR))
GO TO 20
15 DCL=CA/C*(11.5*SIN(DAR)+3.35*SIN(DAR)*SIN(DAR))
DCD=.65*CA/C*SIN(DAR)*SIN(DAR)
CH=CA/C*(CHO-.0542*Y-2.*SIN(DAR))
GO TO 20
5 IF(CS.EQ.0.)GO TO 30
C BEGIN SPOILER INCREMENT CALCULATIONS
IF(17.LT.Y.OR.Y.LT.-17.)GO TO 30
C SPOILER IS ASSUMED INEFFECTIVE FOR POST-STALL CASES
DCL=-9.9*CS/C*SIN(DSR)
DCD=.93*CS/C*SIN(DSR)*SIN(DSR)
IF(0..LT.Y.AND.Y.LE.17.)CH=-(6.7-.175*Y)*CS/C*SIN(DSR)*SIN(DSR)
IF(-17..LE.Y.AND.Y.LE.0.)CH=-(6.7-.075*Y)*CS/C*SIN(DSR)*SIN(DSR)
20 CL=CL+DCL
CD=CD+DCD
GO TO 30
25 CONTINUE
C CALCULATE POST-STALL CONDITIONS FOR AILERON
C CONVERT CL AND CD TO CN AND CC
C
C NORMAL FORCE COEFFICIENT:
C
C CN=CL*COS(ALPHA)+CD*SIN(ALPHA)
C
C CHORDWISE FORCE COEFFICIENT:
C
C CC=CD*COS(ALPHA)-CL*SIN(ALPHA)

```

```

C
C
C
CALCULATE CONTRIBUTIONS TO FORWARD ELEMENT
CN1=CN*(1.-CA/C)
CC1=CC*(1.-CA/C)
C
C
C
CALCULATE AILERON CONTRIBUTIONS
CN2=2.27*2.*PI*SIN(ALPHA+DAR)/(4.+PI*ABS(SIN(ALPHA+DAR)))
DCNA=CN2*CA/C*COS(DAR)
DCCA=CN2*CA/C*SIN(DAR)
CH=-CN2/2.
CN=CN1+DCNA
CC=CC1+DCCA
C
C
C
CONVERT TO LIFT AND DRAG COEFFICIENTS:
CL=CN*COS(ALPHA)-CC*SIN(ALPHA)
CD=CC*COS(ALPHA)+CN*SIN(ALPHA)
30 CONTINUE
RETURN
END

```

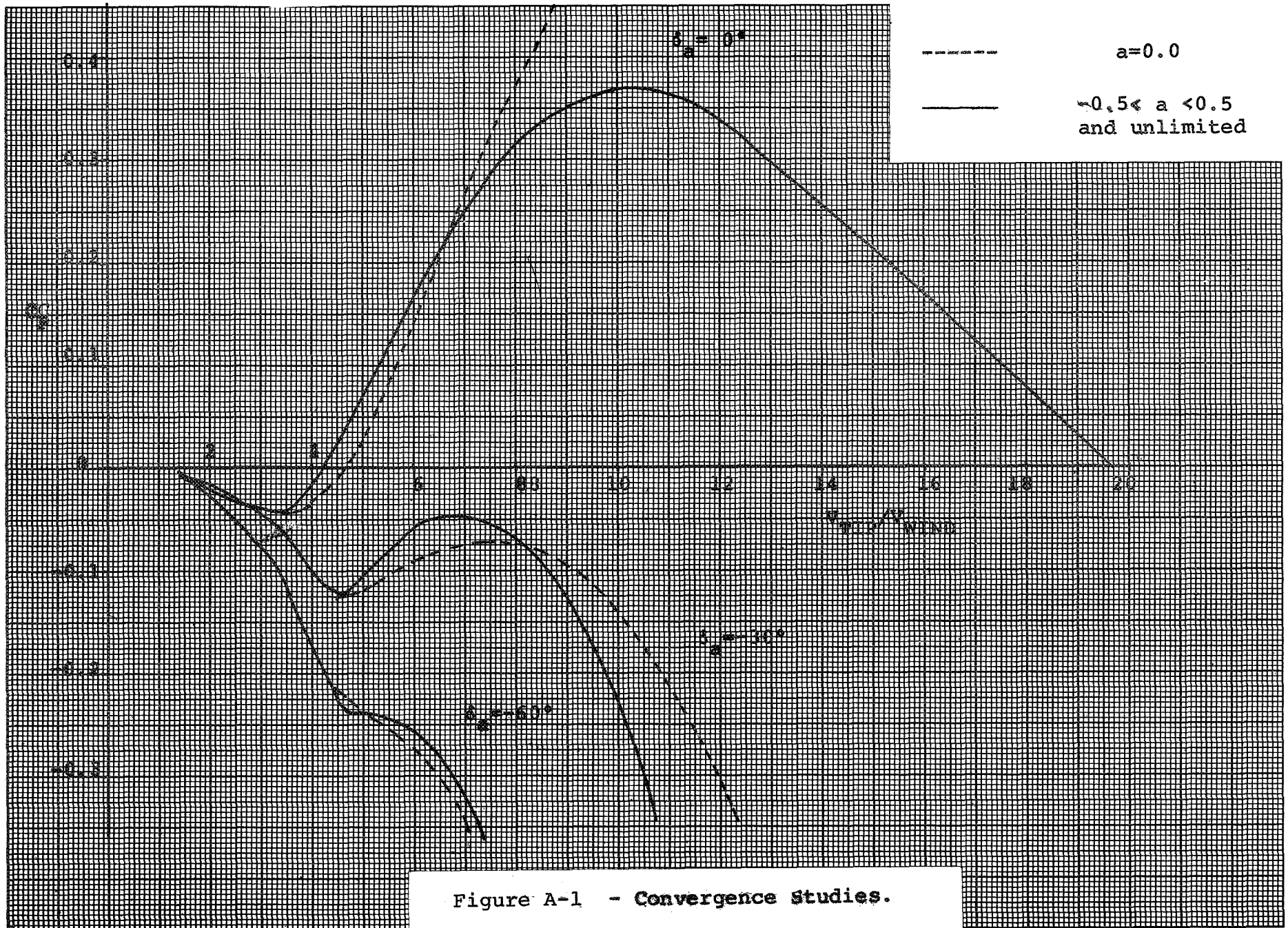
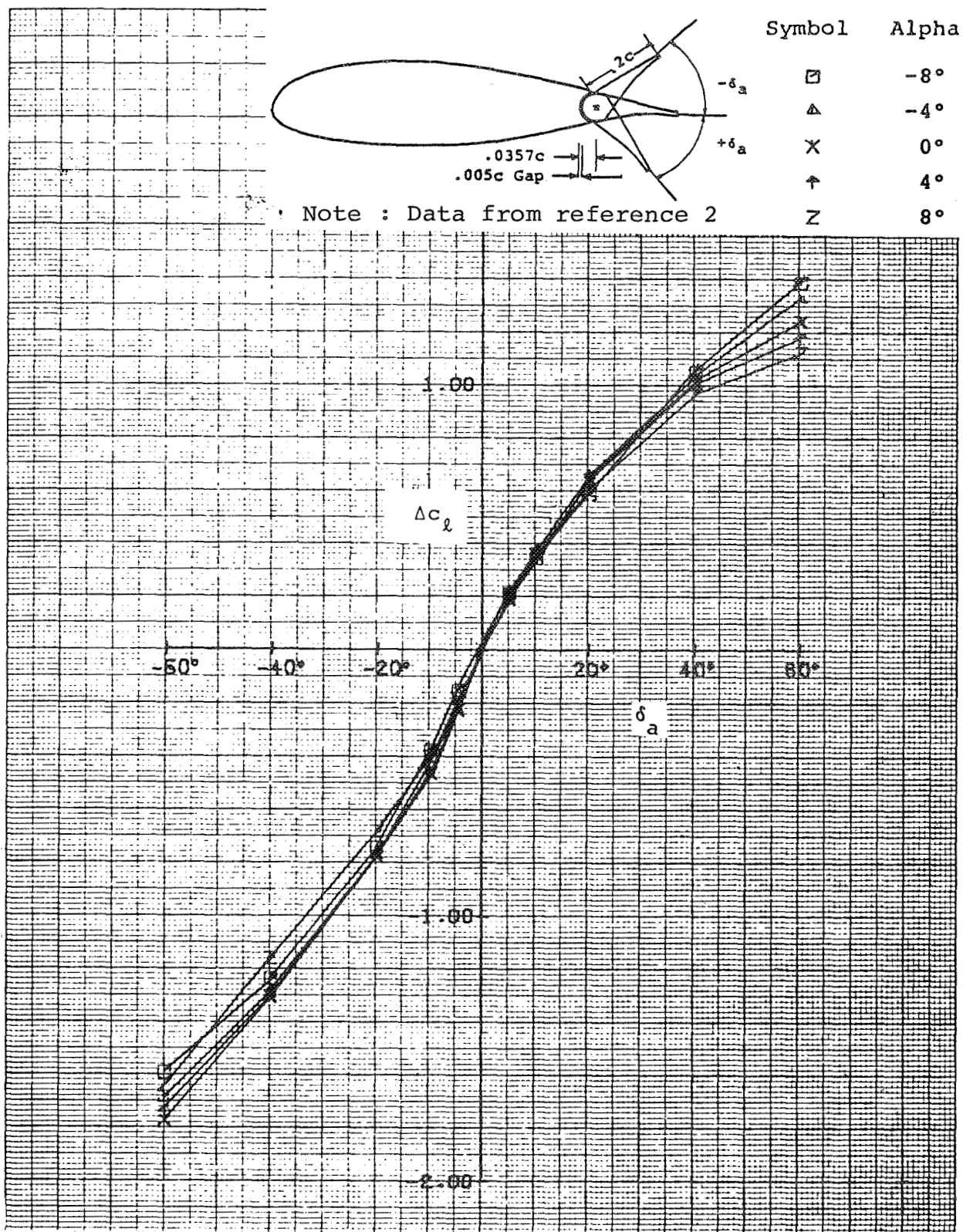
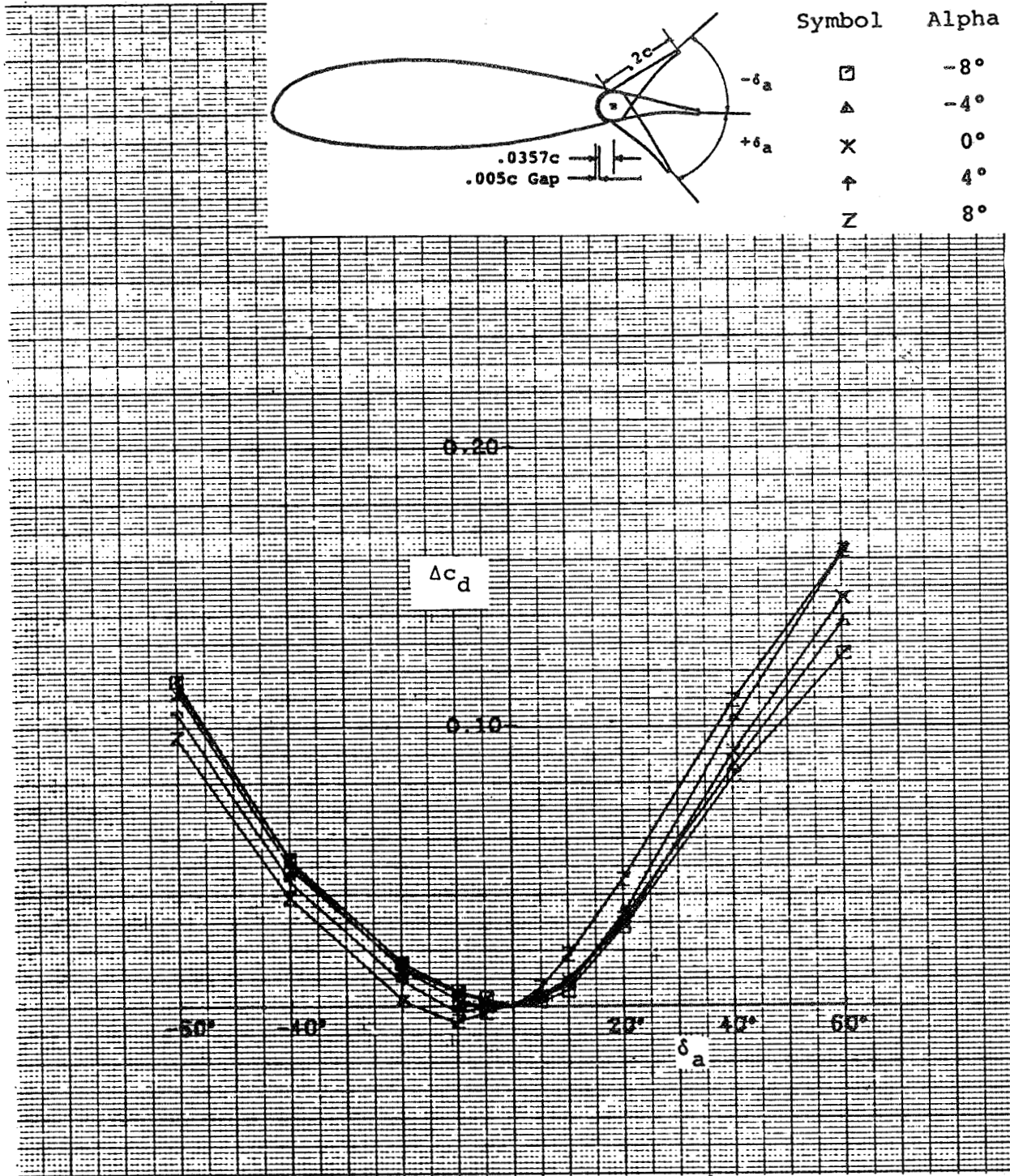


Figure A-1 - Convergence Studies.



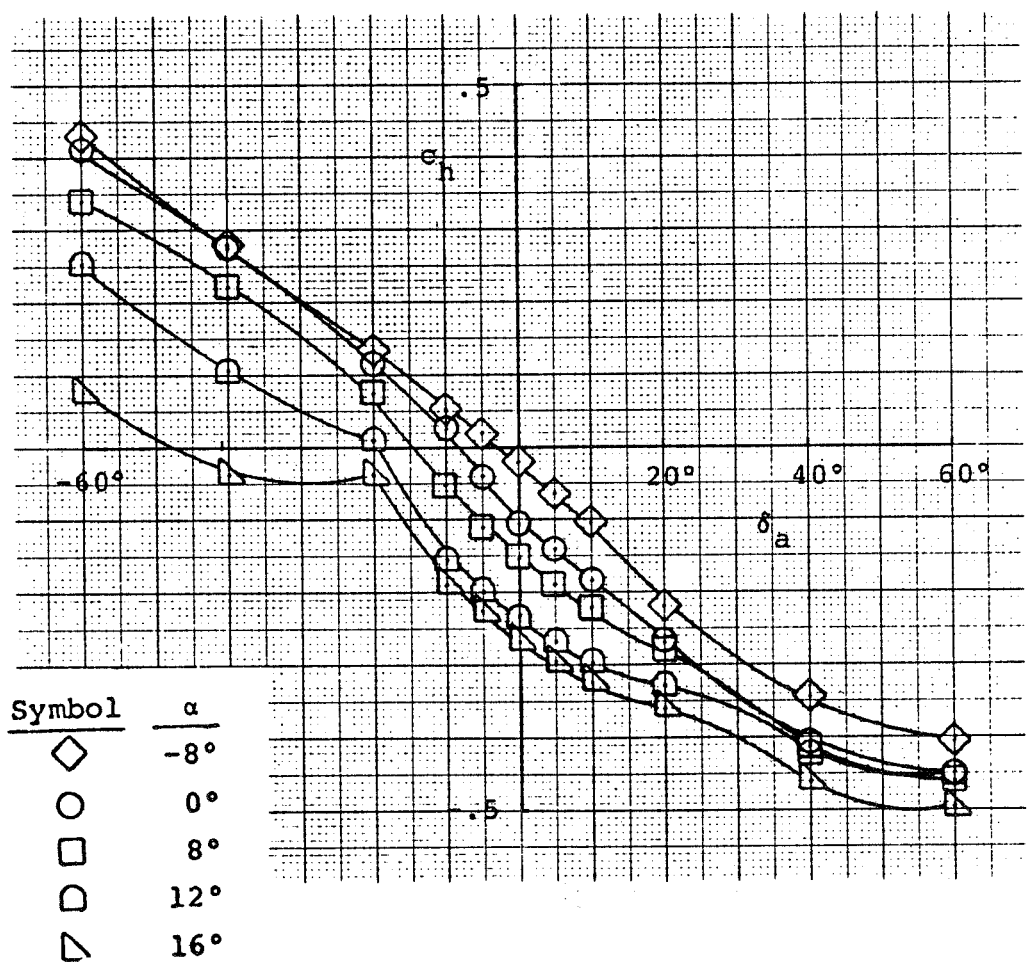
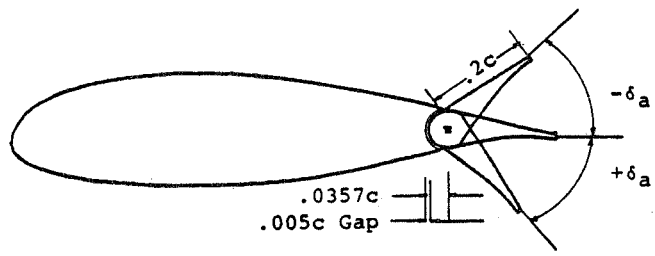
(a) Incremental Lift

Figure A-2 - 20% Aileron Incremental Effects.



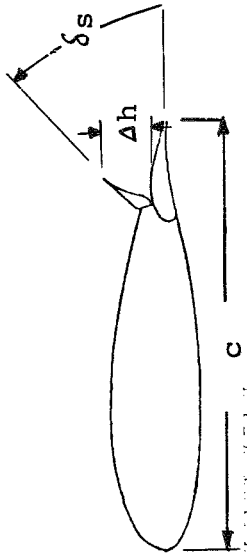
(b) Incremental Drag

Figure A-2 - Continued.

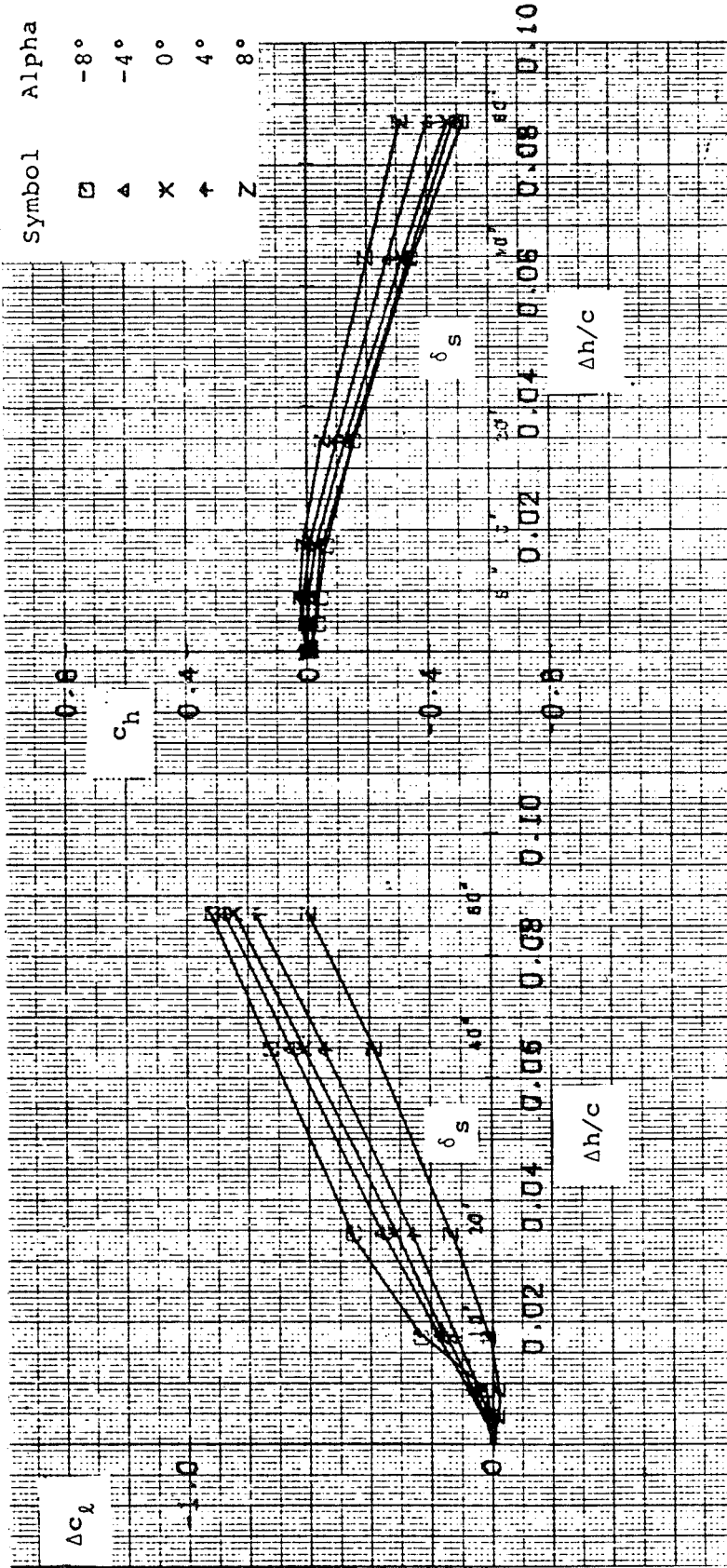


(c) Hinge Moment

Figure A-2- Concluded.



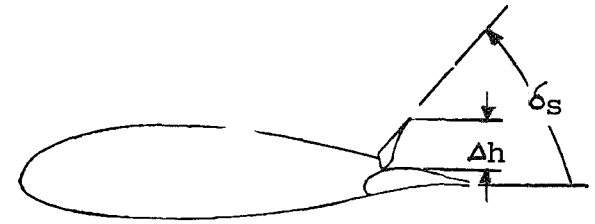
Note : Data from reference 2



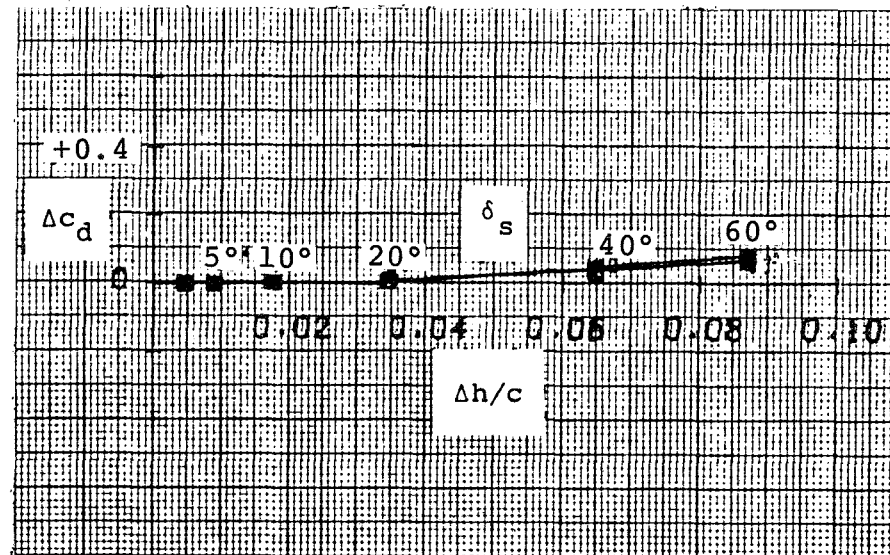
(a) Lift

(b) Hinge Moment

Figure A-3 - 10% Spoiler Incremental Effects.



Symbol	Alpha
□	-8°
△	-4°
X	0°
↑	4°
Z	8°



(c) Drag

Figure A-3 - Concluded.

APPENDIX B

SYMBOLS

a	axial induced velocity factor
a'	rotational induced velocity factor
A	hydraulic piston area, sq in
A _r	aileron rib area, sq in
A _s	aileron skin area, sq in
B	number of blades
c	airfoil or blade local section chord, m (ft)
c _a	aileron chord, m (ft)
c _h	hinge moment coefficient
c _{h0}	hinge moment coefficient at $\alpha = 0^\circ$ and $\delta = 0^\circ$ (a function of camber)
c _{hα}	rate of change of hinge moment with alpha, obtained from the data of reference 5
c _{hδ}	rate of change of hinge moment with aileron deflection, from reference 5
c _l	airfoil lift coefficient
c _n	normal force coefficient
c _s	spoiler chord, m (ft)
c _s	airfoil chordwise force coefficient
c _x	coefficient of force component in plane of rotation
c _y	coefficient of force component in axial direction
C _p	rotor power coefficient, power/ $\frac{1}{2} \rho V^3 \pi R^2$
D	hydraulic piston diameter, in
F	actuating cylinder force, lb
F _C	total centrifugal force on aileron, lb

g	acceleration of gravity, 32.2 ft/sec ²
H	airload hinge moment, in-lb
H _C	hinge moment supplied by centrifugal force, in-lb
K	correction factor, Kirchoff flow
L	length of hydraulic piston travel, in
m	aileron mass, slugs
n	load factor = $\frac{x\omega^2}{g}$
N	aerodynamic normal force, N (lb)
p	hydraulic pressure, psi
q	$\frac{1}{2}\rho(\omega x)^2$, dynamic pressure due to blade motion, N/m ² (lb/ft ²)
r	local blade radius, m (ft)
R	maximum blade radius, m (ft)
t	skin thickness, in
T	aileron deflection torque, in-lb
V	wind velocity, m/sec (mph)
w	weight, lb; also specific weight of aluminum, lb/in ³
w _r	weight of ribs, lb
w _s	weight of skin, lb
x	spanwise distance from center of rotor, m (ft)
X	tip speed ratio, $\omega R/V$
α	angle of attack, deg
δ	deflection angle, deg
ϕ	relative wind angle, deg
θ	blade pitch angle, deg
ω	rotor angular velocity, rad/sec (rpm)

REFERENCES

1. Wenzinger, D.J., and Rogallo, R.M.: Wind-Tunnel Investigation of Spoiler Deflector, and Slot-Lip Lateral Control Devices on Wings with Full-Span Split and Slotted Flaps. NACA Rept. 706, 1940.
2. Wilson, Robert E., and Lissaman, Peter B.S.: Applied Aerodynamics of Wind Power Machines, NSF RANN, Grant No. GI-41840, May 1974.
3. Wentz, W.H., Jr., and Fisco, K.A.: Wind Tunnel Force and Pressure Tests of a 21% Thick General Aviation Airfoil with 20% Aileron, 25% Slotted Flap, and 10% Slot-Lip Spoiler. NASA CR 3081, 1979.
4. Kennard, E.H.: Irrotational Flow of Frictionless Fluids, Mostly of Invariable Density. David Taylor Model Basin Report 2299, 1967.
5. Wentz, W.H., Jr., and Fisco, K.A.: Wind Tunnel Force and Pressure Tests of a 21% Thick General Aviation Airfoil with 20% Aileron, 25% Slotted Flap and 10% Slot-Lip Spoiler. NASA CR 3081, 1979.
6. Abbott, I.H., and Von Doenhoff, A.E.: Theory of Wing Sections. Dover Publications, 1958.
7. Seely, F.B., and Smith, J.O.: Advanced Mechanics of Materials. John Wiley and Sons, 1952.

1. Report No. NASA CR-159856	2. Government Accession No.	3. Recipient's Catalog No.	
4. Title and Subtitle FEASIBILITY STUDY OF AILERON AND SPOILER CONTROL SYSTEMS FOR LARGE HORIZONTAL AXIS WIND TURBINES		5. Report Date May 1980	6. Performing Organization Code
		8. Performing Organization Report No. WER-10	10. Work Unit No.
7. Author(s) W. H. Wentz, Jr.; M. H. Snyder; and J. T. Calhoun		11. Contract or Grant No. NSG 3277	
9. Performing Organization Name and Address Wichita State University Wichita, Kansas 67208		13. Type of Report and Period Covered Contractor Report	
		14. Sponsoring Agency Code DOE/NASA/3277-1	
12. Sponsoring Agency Name and Address U. S. Department of Energy Distributed Solar Technology Division Washington, D. C. 20545		15. Supplementary Notes Final report. Prepared under Interagency Agreement EX-76-I-01-1028. Project Manager, Timothy R. Richards, Wind Energy and Stationary Power Division, NASA Lewis Research Center, Cleveland, Ohio 44135.	
16. Abstract Studies have been conducted to determine the feasibility of using aileron or spoiler controls as alternates to pitch control for large horizontal axis wind turbines. The NASA Mod-0 100 kw machine was used as the basis for this study. Specific performance studies were conducted for 20% chord ailerons over the outboard 30% span, and for 10% chord spoilers over the same portion of the span. Both control systems utilized control deflections up to 60°. Results of the study show that either ailerons or spoilers can provide the control necessary to limit turbine power in high wind conditions. The aileron system, as designed, provides overspeed protection at hurricane wind speeds, low wind speed starting torque of 778 N-m at 3.6 m/s, and a 1.3-1.5% increase in annual energy compared to a fixed pitch rotor. The aileron control system preliminary design study includes aileron loads analysis and the design of a failsafe flyweight actuator for overspeed protection in the event of a hydraulic system failure.			
17. Key Words (Suggested by Author(s)) Wind turbine Aileron Control Horizontal axis		18. Distribution Statement Unclassified - unlimited STAR Category 44 DOE Category UC-60	
19. Security Classif. (of this report) Unclassified	20. Security Classif. (of this page) Unclassified	21. No. of Pages 70	22. Price*

* For sale by the National Technical Information Service, Springfield, Virginia 22161